Thank you to the two reviewers for their positive and detailed reviews. Thank you also to Xuying Liu for her short comment and interest in the paper. We have revised the manuscript accordingly with the following main changes:

- We rephrased *"geolocation"* to *"colocation"*, as reviewer 1 correctly pointed out that the tracks are geolocated with respect to the earth, but we mean a colocation with the initial iceberg outline prior to calving
- We explain our choice to study the B30 iceberg at the end of the introduction
- We changed the colourmap of Figure 1 and 2
- We added more details on the methodology
- We added further discussion including a paragraph on possible causes for iceberg thickness increase
- We added code and data availability statements

Please also see our responses to the specific comments and technical corrections in blue and the tracked changes attached at the end of this document. Line numbers mentioned in our responses refer to the original (Discussions paper) document. We believe that these changes have substantially improved the manuscript. Thank you again to both of the reviewers and Xuying Liu for their comments.

Anonymous reviewer #1:

General comments

The article *"Changes in the Area, Thickness, and Volume of the Thwaites "B30" Iceberg Observed by Satellite Altimetry and Imagery"* presents area, thickness, and volume variations of the iceberg B30 along its lifespan. To get such estimates, the authors rely on different remote sensing products – altimetry from CryoSat-2 and optical and radar imagery from MODIS and Sentinel 1, respectively. The article is, in general, very well written and thorough, and brings new data to iceberg science, a growing field of research. Such data are necessary to better parameterize numerical models that intend to study the role of icebergs in freshwater distribution in the ocean. My most significant comments relate to the author's definition of geolocation, and if this geolocation is indeed worth the extra amount of work given its questionable uncertainties. I conclude that, with a clearer explanation of the methodology and a few corrections, this work will be ready to be published – and will be a welcomed contribution for The Cryosphere.

Thank you for your positive review and your insightful comments on our manuscript – we have addressed each of your specific comments below and think that these changes truly improved the manuscript.

Specific comments

Line 13: What do you mean by *"different modes"*?

CryoSat-2 has three acquisition modes: Low Resolution Mode (LRM), Synthetic Aperture Radar (SAR) and Synthetic Aperture Radar Interferometric (SARIn). We clarified the sentence.

Line 15*: "compare this time series to precisely located tracks using the satellite imagery"* This sentence and the further use of "***geolocation"*** in the paper confuses me. I'm not a person that works with remote sensing, but as far as my understanding goes (please correct me if I'm wrong), altimetry data (at least in its final product) should have latitude-longitude information associated with each data point. And, to my mind, geolocation means using some land feature with known

coordinates in a non-referenced image to infer the lat-lon points in that image. That wouldn't seem to be a problem with altimetry data. From what I have understood from the paper, by "geolocation" you actually mean being able to tell the orientation of the iceberg, so the points over the iceberg are compared with themselves even when the iceberg has rotated.

E.g.: Say you have points **n** and **m** assigned before calving ($t0$); after Δt amount of time drifting, CryoSat-2 measures the height indicated by the yellow "pixel". If you don't know the iceberg's orientation, you could assume the height taken refers to point n (as if the iceberg has not rotated,

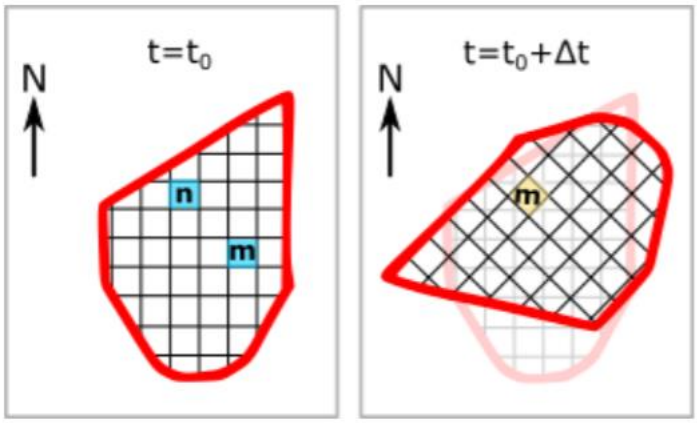

transparent image in the background. But if you to know the new orientation (by "geolocating" the iceberg using imagery), you see that the height measure actually refers to point m.

Did I understand this correctly? Either way, I think this needs to be clarified on the text. I would say something like "determine the iceberg's orientation" instead of "geolocate" or, in case you really mean geolocate, to explain that altimetry data is not referenced to lat-lon positions.

You are correct. What you described is what we meant. We rephrased 'geolocation' to 'colocation' throughout the paper. Thanks for spotting!

Line 26: Very nice overview paragraph!

Thank you.

Line 128: *"(ii) using measurements of the semi-major and semi-minor axes provided by the NIC **and assuming an elliptical shape** and (iii) using measurements of their arc lengths recorded in satellite altimetry **and assuming a circular shape**."* Just to be bluntly clear.

Done.

Line 176: *"to align all images to a common orientation (Fig. 3)".* From my point of view, the common orientation can be seen in Figure 7a-l, not in Fig.3. Unless you are talking about the altimeter track orientation – if so, please specify.

We moved the reference of Figure 3 to another sentence and changed this reference to Figure 7a-l.

Figure 3: There is a O**k**t in figure (a) and a De**z** in figure (c). I'd also indicate which sensor each image is from, which might not be obvious to a person that does not work with satellite data.

Well spotted! We corrected the spelling mistakes and added the sensors.

Line 237: How exactly are you accounting for the iceberg drift? Have you calculated the distance the iceberg has travelled between the CryoSat and MODIS/Sentinel measurements*? And what does this imply? I assume you look at different locations between altimetry and imagery to find the iceberg

(which has drifted between measurements). Or do you take the height measurements from the same points the iceberg is occupying in the imagery, assuming they didn't move but assigning an uncertainty to the drift?

If the image is from a different date than the CryoSat track, we correct the distance travelled based on the daily iceberg locations from the AIT database. In any case, we account for the drift in our uncertainty estimate, which is higher the larger the time separation is. We added this explanation in the paper to clarify.

*In model simulations, the icebergs' average speed is 0.14 m/s, which means it would have moved around 500 m in 1h.

Then, you assume that the iceberg has kept the same orientation but account for an error of 15°/day. How do you combine all those uncertainties to get to a final error in the freeboard estimate? Could you include an equation or give more detailed information on the supplementary material?

We updated the text to make this clearer. Our drift speed of 3 km/day is based on findings by Scambos et al. (2008), who find a net movement of approximately 2–3 km/day south of 65 degrees South in free-drifting periods for two icebergs with GPS stations installed on them.

Although the methodology is, in general, very well described, I'm not sure about this part. And that makes me wonder if using the imagery to infer spatial height variability (assigning the altimetry data to specific points on the iceberg) is worth the trouble. I see that the final variability is reduced when this procedure is done (compared to the averaged freeboard estimate) on line 340, but as you mention, this is probably the case because the iceberg has a "homogeneous thickness", i.e., if you mistake one grid cell for another it is not a big deal. And, if the thickness is homogeneous, then the averaged height along the track (without "geolocation") should be good enough – which indeed is the case, since you mention that the different methodologies' results are in good agreement. So, maybe this "geolocation" is more useful when one is dealing with a non-tabular iceberg, where the thickness from point to point varies a lot and doing simply a freeboard average along the iceberg would lead to the significant loss of spatial information. However, in this case, the uncertainties brought by the time difference between the altimetry and imagery would be much more damaging to final results, since mistaking one point of the iceberg for another would imply much larger errors.

You are right. For this iceberg we find that colocation improves the uncertainty only slightly, but to generalise this finding more icebergs with different topographies would need to be studied. The Thwaites Ice Shelf is also particularly rugged and crevassed, which leads to high variations within the same grid cell. For other icebergs with more heterogeneous freeboard across the iceberg that are less crevassed, colocation might have a larger impact. We added these explanations to the text as well.

Line 253: I assume by thickness you mean draft + freeboard?

Correct. We clarified this in the paper, too.

Line 267: Define SWE.

Done.

Figure 7: The caption needs to be updated with the subplots' correct letters.
*"**m)** mean difference of each new overpass along time."*
*"**a-l)** freeboard difference in each grid cell"*

Done

Also, in a-l, the Δt is indeed always positive? i.e., is the satellite image taken always after the CryoSat overpass? If not, you could differentiate them with a minus sign for images taken before the CryoSat overpass.

Good idea to differentiate between images taken before and after CryoSat. We updated the numbers in the figure. We also noticed that the time differences given in the figure so far were only approximate and based on the times from the CryoSat file names. In the calculation and for the new updated time differences, however, we use the time of the overpass over the iceberg, which is up to 1.5 hours later and describes the offset to the image more accurately.

Figure 8: (a), (b), (c), and (d) labels missing from plots

Done

Line 376: I'd actually move the reference to Figure 8d to the next sentence:
*"This amounts to 117 ± 38 m of thinning **(Fig 8d**)"*

Done

Line 391: Fig 8d actually shows the thickness **differences**

True. We deleted the reference here.

Line 400: "*volume changes due to fragmentation become the dominant source of ice loss towards the end of our survey".* Isn't that funny, though? I'd imagine it is much easier to break a large piece of ice than a small one. And it even somewhat contradicts what was said in line 57: "breakage dominates over melting for large icebergs". Could you offer an explanation, then, why fragmentation becomes more important at the end of this iceberg's life?

A similar behaviour has also been reported in other studies (Bouhier et al., 2018; Scambos et al., 2008). The main drivers of fragmentation are surface melting, which can lead to a rapid disintegration (Scambos et al., 2008) and wave erosion or wave stress (Wagner et al., 2014) which increase the further North (i.e. surrounded by open ocean and warmer air temperatures) the iceberg gets. Even at the end of this study period, the B30 iceberg is still considered a very large iceberg (it still has a long axis of 35 km according to the NIC). In a model used by England et al. (2020) for example icebergs break up as long as they are at least ~900 m long. We added a sentence to discuss this in the paper, too.

Line 406: A relevant reference here is Martin and Adcroft (2010) when talking about bergy bits.

Thank you. We added the reference here.

A note about the colormaps used in the figures: although I do enjoy rainbow colormaps, it is good to think about inclusion – namely, colorblind readers. Even for me, the colormap in Figure 1 and 2 could get confusing: it starts with red and finishes with… red. Of course, we infer which color corresponds to which year just by following the progression of the iceberg, but that should be clear from the color scheme as well. The colormap in Figure 4c and 4d is a good one: starts with bright colors, finishes with dark ones. When in doubt, there are resources such as:
https://www.color-blindness.com/coblis-color-blindness-simulator/
where you can upload you figure and see how it looks like for someone with color vision deficiency. Also, I prefer discrete color bars rather than continuous ones, so you can really see what values are

attributed to each color. I don't expect you to change all your figures now, but I wanted to throw the idea out there to keep in mind for next publications.

Thank you for your thoughts and the reference. We changed the colourmaps of Figure 1 and 2.

Technical corrections

Line 27: Be mindful of commas. I found them missing from some places, but there could be more around. Here: "*At any time, (…)".*

Done

Line 34: Check if there is a space between *"production"* and the following parenthesis.

Done

Line 56: *"iceberg melting, to first order, (…)"* or rearrange the sentence such as *"found that iceberg melting is proportional to water temperature to first order (…)".*

Done

Line 71: *"also included"* – just to be consistent with "*studied"* in line 70.

Done

Line 73: *"employed altimetry measurements"* – same as above.

Done

Line 125: *"The initial area"* (also, could you provide the length of the iceberg?)

Done. Yes, we added this: The iceberg's initial length was 59 km according to the National Ice Center.

Line 74: *"Bouhier et al. (2018) analysed*" – same as above; plus, that's a long sentence. I'd just split it into 3 shorter ones, one for each citation.

Done

Line 75: *"(…) geolocation. Li et al. (2018) calculated"*

Done

Line 76*: "(…) overpasses. Han et al. (2019)"*

Line 78: "*When thickness and area changes are combined, it is possible (…)*"

Done

Line 174: *"CryoSat-2 overflights.*" – the end of this sentence doesn't read well, so you can just remove it.

Done

Line 287: Maybe *"less accurate*" would sound better than "*more approximate*"

Done

Figure 6: On the caption: *"over time (a) and as scatter plot (b)."*

Done

Line 315: *"larger sections ~~and~~ more rapidly*."

Done

Line 320: *"In 2018, (…)"*

Done

Line 341: Do you mean Figure 7m instead of 5a?

Yes, corrected.

Line 393: *"To compute changes in mass, we (…)"*

Done

Line 412: "*thickness, and volume (…)"*

Done

Reviewer #2 (Jessica Scheick):

General Comments:

The manuscript tracks Antarctic iceberg B30 using satellite imagery and altimetry observations. The authors utilize these observations to determine changes in iceberg area, freeboard, and volume through the iceberg's drift from its calving location from the Thwaites Ice Shelf. Their analysis investigates the viability of using semi-automated methods for estimating iceberg area, the importance of geolocation in estimating iceberg freeboard, and the impact of including snow accumulation and snow and ice density variations in computations of ice thickness.

This work contributes to our ability to scale up analyses of iceberg drift and disintegration by quantifying the limitations of some common assumptions and uncertainties of various methods, especially as they relate to semi-automating the analysis. However, it would benefit from a more thorough exploration of these assumptions and discussion of where future work should focus on improvements. A few key areas of focus for improvement prior to publication are:

Thank you for your detailed review and the time you put into it. We responded to all of your comments below and hope this clarifies our work further and resolves the misunderstandings.

1. Overall clarify and improve the motivations and contextualization within the literature. What is unique about this investigation? The novel contributions of this work (investigating the influence of geolocation on iceberg freeboard estimates; including snow accumulation and density variations in thickness calculations) only become clear towards the end of the manuscript. Many areas of the methodology and discussion are lacking citations and explicit connections between previous results and this investigation (a few specific cases are pointed out in the line comments, below, but this list is not exhaustive). Why did you choose to focus on iceberg B30? What should we take away from this investigation, and how should it inform our future work? What are the critical next steps needed to further this work?

   This is quite a challenging and dispiriting opening series of comments. The main novel contributions of our study are all mentioned in the abstract; not overstating their novelty explicitly is our preferred writing style for a study of this nature. We have though tweaked

the paper title to be a little more emphatic, we have added reference to our use of meteorological data in the abstract, and we have added a few sentences at the end of the introduction to restate the novel contributions and to explain our choice of B30 as a test case and the significance of the berg itself. We also don't agree that there is a lack of citation; we cite 59 papers in total which is towards the upper limit (80) for the journal and significantly higher than the upper limit for many other journals, and we have provided specific responses to the related comments. Finally, the take-away messages and future work are already mentioned in our conclusions. We note that none of these concerns relate to the scientific contribution of our study, which leads us to believe that we may have misunderstood their intent.

2. Clean up precision of language, passive voice, and extraneous phrases ("more recently, for example"). This includes separating run-on sentences and connecting ideas throughout and between paragraphs (there are a few abrupt transitions and locations where critical information is presented a page or two later than the reader needs the information).

   We corrected the language and the abrupt transition.

3. Closely examine the text for statements that need further quantification, explanation, citation, etc. This is similar to 1 and 2, but refers to particular statements like "While manual delineation provides the most consistent and accurate area estimate" or "boundary detection techniques" or "large" icebergs or iceberg "area" and "thickness". Additional details on your approach, methods, and definitions will convince the reader they agree with your interpretations and make your method reproducible.

   We added more details on the methods, explicit definitions for area and thickness, and used the word 'significantly' more carefully. Please also see our responses to the related specific comments.

4. Data and code access. The manuscript does a reasonable job of outlining what computational tools are used but does not provide enough details to make the study reproducible nor indicate where readers can get more information. What software and data versions are you using? What corrections did you apply? Is your code publicly available? Why or why not? Are the iceberg polygons available?

   Thank you for spotting this. We added code and data availability statements. The corrections applied, software and data products are mentioned in the methods section (e.g. lines 121, 135-140, 186, 188, 191-192, 197, 199-201, 220-229, 237-238, 263-266, 270, 281-282) and acknowledgement (lines 242-244). For the AIT database we added the version number and for the CryoSat-2 data we added the baseline. For MODIS, Sentinel-1 and the ERA-5 data there is only one version available and no specific version numbers are given in the archives.

Specific ("line") comments:

Abstract:

p1 Line 15: You're comparing a time series to a geospatial track?

We clarified this in the paper.

p1 Line 18: geolocation of imagery reduces the uncertainty of what by 1.6 m? Iceberg location? Freeboard?

Freeboard. We clarified the sentence.

Introduction:

p2 Line 52: “ice shelf barriers” = “ice shelf fronts”? I think this may be a British/American English difference, since I’d previously only heard this term in reference to Ross Ice Shelf

The term “ice shelf barrier” refers to the role of the ice shelf as an interface between the ice sheet and the ocean and not just the specific calving front (although of course all barriers have a “front”). For a recent discussion see the reference cited (Shepherd et al., 2019).

p2-3 Lines 55-56: be careful not to mix terms: melting and breakage are both forms of mass loss

We rearranged the sentence to avoid misunderstandings.

p3 Line 65: Explicitly state your focus on tabular Antarctic icebergs, versus icebergs generally

We study a tabular Antarctic iceberg (mentioned e.g. in line 11 and added to the title now), but we think the statement *“The advent of satellite remote sensing greatly increased our capability to study icebergs.“* holds for smaller icebergs, too.

p3 Line 83: the studies cited here occurred before the ones cited in the previous sentence…

We changed the sentence.

p3 Line 85: this is an abrupt transition. Also, is your method less labor intensive?

We added a paragraph to mitigate the abrupt transition. In our experience, producing elevation data from stereo-photogrammetry and interferometry are certainly labour intensive by comparison to satellite altimetry. The text was updated to clarify.

Iceberg location:

p4 Line 103: longer than 6 km in what dimension (their longest? How is this estimated?)

6 km refers to the long axis. We believe that they track icebergs, which are visible in their scatterometry data. For more details please see Budge & Long (2018).

Initial iceberg shape, size and calving position:

p6 Line 126: The initial area may be more appropriately reported in the next subsection.

As the initial shape and area are derived from the same polygon, we decided to state them in the same subsection.

Iceberg area:

p6 Line 128: please clearly define “iceberg area”. I am assuming for the purposes of this review that “area” refers to the two-dimensional, plan-view, non-submerged portion of the iceberg

Your assumption is correct. We also clarified this in the paper.

p6 Line 130: I would like to see some justification for the statement that manual delineation provides the most consistent and accurate area estimates. From my experience, selecting consistent iceberg boundaries manually is non-trivial and can result in multiple “correct” delineations with vastly different areas. The introduction of multiple operators can further increase the spread of possible surface area estimates.

In our results section and Figure 6 we show that manual delineations are much more consistent and realistic than the other approaches. As you say even manual delineations come with an uncertainty. We account for this in our uncertainty estimates.

p6 Line 137: Please include which orbital and radiometric corrections you’re using.

We apply precise orbit files and the radiometric corrections provided by the calibration Look Up Tables in the Level-1 products using the ESA SNAP software. For more information please see the hand book or help of SNAP, which is an open source software.

p6 Line 144: What boundary detection techniques do you use? How do you select any parameters used in these techniques, and how do these affect your area estimates?

We use matlab’s bwboundaries function, which implements the Moore-Neighbor tracing algorithm modified by Jacob's stopping criteria. As we only use a limited number of area outlines, we haven’t experimented with different techniques or parameters and simply use manual delineations when this method fails. We added more details in the paper, too.

p6 Line 146: What “rules” (explicit or implicit) are you using during manual delineation? Shadows cast on the sea ice? Texture differences? How do you handle areas that are “blurry”?

If areas are blurry due to cloud cover, we use multiple MODIS images together, where different parts are covered by clouds. Mostly the colour (or grey scale backscatter for Sentinel 1) is enough, but in some MODIS scenes where the iceberg is surrounded by sea ice, you can also detect a texture difference when zooming in (e.g. Fig. 3b). We also clarified this in the paper.

p6 Line 147: What shape kernel do you use for the shrinking and expansion?

We did not use a kernel, but simply moved each polygon point by one pixel (lines 146-147).

p6 Line 148: What is the standard deviation on this mean relative difference?

We added the standard deviation of 0.9 % to the paper.

p7 Line 157: How are the NIC axes determined? If this is done manually (as stated in line 160), then you cannot argue this approach is less time consuming or subject to individual judgement (line 156).

NIC axes are indeed derived manually, but we think it’s much faster to measure two axes than clicking the whole outline (‘delineation of their full perimeter’, line 154). Furthermore, this is an

operational service (line 158) and therefore it saves time for end users, who don't have to duplicate their work.

p7 Line 163: Can you compare one of your area estimates to one of the elliptical ones from NIC and combine the area datasets?

We compare our estimates to the estimates of semi axes by NIC assuming an elliptical shape in Figure 6 and section 3.1. A direct comparison is shown in the scatter plot (Fig. 6b).

p7 Line 166: How are iceberg arc lengths determined from CRYOSat-2 data? Is this an existing product or are you deriving the iceberg arc lengths?

We are deriving the arc length from the same tracks that we use to estimate the freeboard and thickness. This was clarified in the paper.

p7 Line 168: Please provide additional information on the "significant variations" in area estimates from your third method.

We rephrased 'significant' to 'considerable'. What we mean is that the area estimates based on one arc length are not consistent and vary depending on where the CryoSat track crosses the iceberg.

p8 Line 169: what dimension is the moving mean computed across?

It's computed along time and this was added to the paper.

Iceberg orientation:

p8 Line175: is the rotation performed manually or automatically?

The rotation angle is adjusted manually.

Initial iceberg freeboard:

p9 Line 198-201: Were the outliers removed sequentially using the filters described (i.e., were the median and mean filters applied to the range of freeboard heights subsequent to the removal of values outside the 20-60 m range?). Also, with median it is customary to use standard absolute deviation, rather than standard deviation. What criteria were used to select the 20-60 m initial filter, and could similar removal of outliers be accomplished with only one or two median or mean filters?

The filters were applied successively. 20-60 m are based on the findings by Tournadre et al. (2015) and ensure that all remaining measurements are actually from the iceberg (lines 223-224). This step is important, because including returns from e.g. nearby land, sea ice or simply outliers could bias the mean and median. We added the reference here, too.

p9 Line 202: What criteria are used to detect and exclude crevasses?

The filters described above are used to exclude crevasses. We clarified this in the paper.

p9 Line 209: Be aware of using "significantly" without quantification.

We rephrased "significantly" to "considerably".

Iceberg freeboard change:

p10 Line 220+: It's unclear exactly what filtering is done here to extract icebergs. Is land excluded geospatially, or is it excluded using one of the height filters? It might help the reader to be explicit that you are automatically extracting iceberg freeboards from tracks, motivating the need for multiple filtering steps.

Yes, we exclude land using these height filters, because land masks are not accurate enough along advancing and retreating ice-shelves and the iceberg is drifting very close to the ice-shelf margins occasionally. We also added a sentence to point out that we are automatically extracting the iceberg from the tracks with these steps.

p10 Line 226: The editing steps to remove rugged features and crevasses are not previously described (as such).

They are described in lines 193-201.

p11 Line 248: If you were to compute an iceberg freeboard for the pre-calved iceberg using just one of the tracks used in your compilation, how would that value compare to the mean freeboard calculated using the composite? Making this comparison would be a compelling way to show that your mean along-track freeboard computations can be directly compared to the mean surface height prior to calving as a measure of changes in freeboard.

This is indeed a nice idea for validation! We made this calculation for each of the 15 tracks over the pre-calved iceberg and find a standard deviation of 2.8 m compared to the mean initial height of 49.0 using all the tracks. This was also added to the paper.

Iceberg thickness:

The equations presented in this section are described in the text but are not incorporated into it. Instead, they hang between paragraphs. Constants used within the equations should be explained and/or cited.

We double-checked and couldn't find any constant that was not explained.

Results and Discussion:

p16 Line 343-345: The reader could benefit from this information on the variability of freeboards being presented earlier in the manuscript.

We also presented this information in line 206.

Iceberg thickness change:

p17-18: this section presents a lot of critical information but is rather confusing because it switches between negligible and non-negligible influences on iceberg thickness and density. Please revise to flow logically and indicate which processes were considered and which were included in the final calculations.

We arranged this section based on the different parameters, therefore e.g. firn densification comes after ice density changes and snow melting comes after snow accumulation.

All processes that are mentioned in the methods section were included in the final calculation. The other processes with negligible influence are only shortly mentioned here as a discussion. We made it more explicit in the paper that the effect of surface melting is not applied. For firn densification this is already stated (line 365).

p18 Line 366: Is the snow density averaged vertically, assuming a uniform horizontal thickness?

We directly calculate the mean snow density; it's not explicitly averaged vertically (Line 255: ρ_s is the column-average snow density). Only for the ice density we model the density profile.

p18 Line 369: where were above-freezing degree hours calculated?

We mention how it's calculated in this line. The data (2m air temperature data) was introduced in section 2.7. Or do you mean where geographically? It's calculated along the iceberg's trajectory.

p19 Line 377: Is a linear, annual average the most representative of iceberg processes?

Icebergs are not melting linearly and at a constant rate, but this allows us to compare our work to previous studies and set the findings into context (line 377 onwards).

p20 circa Line 385: The authors clearly articulate and demonstrate the importance of including snow accumulation in thickness computations. It would be great to see some further discussion of this. Some potential avenues for exploration include noting over what temporal and/or spatial scales (e.g. when the iceberg is close to the coast) these effects are important, recommendations for when this is a critical component that should be included in estimating iceberg thickness, and or discussing the limits of including snow accumulation but excluding wind scour and other snow removal processes.

Figure 8 suggests more or less linear snow accumulation. The influence of the snow layer is probably larger when the iceberg is melting less and becomes larger the longer the iceberg survives. For a real judgement, more icebergs in different environments need to be accessed, though. We added a short discussion on this in the paper.

Iceberg volume and mass change:

p20 Line 389-390: This line is a great example of a clear, simple statement that provides information about your logic/assumptions and objectives. Awesome!

Thank you.

p20: What are the implications of your assumptions about shape on volume? This is a critical assumption in estimating iceberg volume that has been quantified (to the best of our ability) and discussed in the literature (e.g. Enderlin and Hamilton 2014, Sulak et al 2017, Schild et al 2021, and many others). Your discussion needs to address the assumptions you've made and justify the interpretation on the results accordingly.

Iceberg shape plays a role for small icebergs. However, large tabular icebergs like B30 inherit their shape from their parent ice shelves and therefore have rather homogenous thickness and near vertical walls. So, they are treated as prisms with constant area from the surface to the base. B30 for example was 59 000 m long and 315 m thick at calving and had a length to thickness ratio of 187:1. Slightly tilted sides have minor effects on the total volume and we anticipate that the deviations from vertical occur in both directions, so they approximately even out across the whole side surface

(e.g. Orheim, 1987). We therefore don't regard a discussion of iceberg shape as relevant for a tabular iceberg of this size. The papers you mention all refer to small icebergs with totally different dimensions and are not transferable to large tabular icebergs.

Since you brought this up, we, however, did a few quick calculations using the formulas from Enderlin and Hamilton 2014 and simple trigonometry (see below). These show that the B30 iceberg would need near horizontal side walls (tilted by 1.5 degrees compared to horizontal) in order to have a conical shape. This seems very unrealistic.
If all sides were tilted by 5 degrees compared to vertical this would lead to a 0.1 % difference in volume and an absolute difference of 0.6 km^3 compared to an uncertainty of 57 km^3 (line 398). These results confirm that deviations from our prism assumption with constant area have negligible impact on the volume of this tabular iceberg.

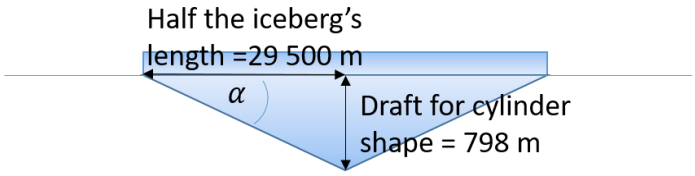

→ α = 1.5°

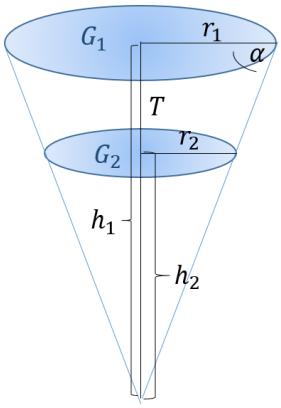

$G_1 = 1500\ km^2$ ..*iceberg area*

$T = 0.315\ km$ ..*iceberg thickness*

$\alpha = 85°$

$r_1 = \sqrt{G_1/\pi}$

$h_1 = r_1 \cdot \tan(\alpha)$

$h_2 = h_1 - T$

$r_2 = h_2/h_1 \cdot r_1$

$G_2 = r_2^2 \cdot \pi$

$Volume = \frac{1}{3} \cdot (G_1 \cdot h_1 - G_2 \cdot h_2) = 471.9\ km^2$

$Volume\_cyl = \frac{1}{3} \cdot (G_1 \cdot T) = 472.5\ km^2$

} $Difference = 0.1\ \%$

p20 Line 407: Do you calculate freshwater flux? If not, why?

We can only give a lower bound estimate of the freshwater flux, which is the volume loss due to basal melting of the mother iceberg. As the fragments, which are lost from the sides, are not tracked by the database and most of them are too small to be tracked by altimetry, we can't say how quickly they melt and therefore how much they (and hence fragmentation) adds to freshwater flux. This is also discussed in the paper (Lines 404-407).

Figures (overall):

What uncertainties are shown (two sigma?)

The uncertainty of freeboard is one standard deviation. This was added to the figure caption. The other uncertainties shown are estimated as described in the methods.

Figure 1: Why is there such a large data gap circa 2018-2019?

It's a data gap in the Antarctic Iceberg Tracking database.

Figure 2:It would be helpful to have the icebergs in panel (b) oriented as they are in panel (a). Is the orientation of all of the depictions in panel (b) with north to the left? What is the influence of outline complexity on area? there is a very clear difference between the level of detail in the iceberg outlines that were manually derived versus the edge detection derived outlines.

The icebergs in panel b are depicted in a polar stereographic projection (information added to the caption). We didn't investigate the influence of outline complexity on area systematically, but there were a few instances where we first clicked the outline manually and then discovered the automatic technique and we remember that the difference was small compared to the total area.

Figure 3: Can you really see the iceberg orientation in panel (l)? Also, why doesn't the initial iceberg fully encompass the iceberg depicted in later panels? This suggests to me either the initial iceberg outline needs to be modified or the rotational alignment should be improved.

For example in panel b the iceberg has sea ice frozen to its side. When you zoom in, the sea ice is slightly transparent/darker and has a different texture than the iceberg. Using a sequence of several images helps to identify this. In panel l zooming in and using several images in combination, where the clouds cover different parts of the iceberg helped to identify it. This is definitely our worst quality image, though. The following image was taken only one day later and really helped to find the iceberg in the image from the previous day. We clarified this in section 2.3 in the paper.

Figure 4: It's interesting that one of the areas with the largest number of observations is also one of the areas with a comparatively higher standard deviation. Is this a particularly complex or crevassed region?

We can't judge, but this is indeed what the figure suggests.

Figure 5: This figure is immensely helpful for visualizing your workflow. It might be helpful to the reader to isolate some of the filtering steps to illustrate why each one is needed (perhaps as a supplementary figure?).

The figure separates the main two steps: 1. Identifying where the iceberg is (blue) within each track (black) and 2. Which parts of the iceberg (blue) are crevasses (remaining heights in red).

Figure 7:Why does the difference in freeboard have such a potentially large positive range (it appears there are no values larger than about 7 m)? Plots are mislabeled relative to the caption. What is the shaded region showing? Label the axes in plot n. How do you explain the large variability (specifically the increases in freeboard)?

Do you mean why our y-axis ends at +15 m? This is to show the whole uncertainty range (shaded region), to leave room for the legend and because we wanted to have a y-axis label at the upper end (labels every 5 m). Mislabeling was corrected. Thanks for spotting this.

The increase in freeboard and thickness is indeed very interesting. We added a paragraph to discuss the possible causes. For more details, please see our response to the short comment from Xuying Liu below and the tracked changes.

Grammar:

- Heading titles have inconsistent capitalization

  Corrected

- inconsistent use of Oxford comma

  Corrected

- watch for possessive apostrophes (both missing and extraneous)

  Corrected

- p16 Line 341: there is no (a) in figure 5

  Corrected (see reviewer 1)

Short comment (Xuying Liu):

Thank you for your work on iceberg thickness and volume changes of B30.

I've got a question while reading. Figure 8(d) shows a significant trend of thickness descending from 2012 to 2018. But there's also some rises of thickness shown by the figure. What may cause the iceberg being thicker during its drift? It would be appreciated if you could share your opinions.

We added the following paragraph to discuss this in the paper:

"Besides the observed thinning, the iceberg also seems to slightly thicken between mid-2014 and early 2015. During this time B30 was very close to the coast (Fig. 3b-d). Therefore, a range of processes – both physical processes that impact the actual thickness of the iceberg and processes that impact the freeboard measurement – could have caused this gain in thickness: First of all, iceberg thickness can increase through marine ice formation, when the iceberg is surrounded by very cold water. It can also grow through snow accumulation on the surface, which we account for, but only based on reanalysis data and there might be additional local snowfall or snow accumulation through strong katabatic winds from the near-by continent. Furthermore, external forcing from fast ice and/or collisions with the adjacent ice-shelf might have led to a deformation and hence a compression in some parts. All of these processes can cause a physical increase in iceberg thickness. Apart from that, a short (partial) grounding could lead to higher measured iceberg freeboards. Also surface melting could shift the scattering horizon of CryoSat-2 and therefore appear like a freeboard increase. Indeed we observe a steep increase in degree hours around the turn of the year 2015.

What caused the signal in this instance is hard to disentangle. Most probably, it was a combination of several of the mentioned effects.”

Tracking Changes in the Area, Thickness, and Volume of the Thwaites ~~'B30'~~ Tabular Iceberg 'B30' ~~Observed~~ using ~~by~~ Satellite Altimetry and Imagery

Anne Braakmann-Folgmann[1], Andrew Shepherd[1], Andy Ridout[2]

[1] Centre for Polar Observation and Modelling (CPOM), University of Leeds, Leeds, LS2 9JT, UK
[2] Centre for Polar Observation and Modelling (CPOM), University College London, London, UK

Correspondence to: Anne Braakmann-Folgmann (eeabr@leeds.ac.uk)

Abstract. Icebergs account for half of all ice loss from Antarctica and, once released, present a hazard to maritime operations. Their melting leads to a redistribution of cold fresh water around the Southern Ocean which, in turn, influences water circulation, promotes sea ice formation, and fosters primary production. In this study, we combine CryoSat-2 satellite altimetry with MODIS and Sentinel-1 satellite imagery and meteorological data to track changes in the area, freeboard, thickness, and volume of the B30 tabular iceberg between 2012 and 2018. We track the iceberg elevation when it was attached to Thwaites Glacier and on a further 106 occasions after it calved using Level 1b CryoSat data, which ensures that measurements recorded in different acquisition modes and within different geographical zones are consistently processed. From these data, we mapped the iceberg's freeboard and estimated its thickness taking snowfall and changes in snow and ice density into account. We compute changes in freeboard and thickness relative to the initial average for each overpass and compare these~~is time series~~ to estimates from precisely located tracks using the satellite imagery. This comparison shows ~~that our time series of iceberg freeboard change is in~~ good agreement ~~with the geolocated overpasses~~ (correlation coefficient 0.87), and suggests that ~~geolocation~~ colocation reduces the freeboard uncertainty by 1.6 m. We also demonstrate that the snow layer has a significant impact on iceberg thickness change. Changes in the iceberg area are measured by tracing its perimeter and we show that alternative estimates based on arc lengths recorded in satellite altimetry profiles and on measurements of the semi-major and semi-minor axes also capture the trend, though with a 48 % overestimate and a 15 % underestimate, respectively. Since it calved, the area of B30 has decreased from 1500 +/- 60 to 426 +/- 27 km^2, its mean freeboard has fallen from 49.0 +/- 4.6 to 38.8 +/- 2.2 m, and its mean thickness has reduced from 315 ± 36 to 198 ± 14 m. The combined loss amounts to an 80 +/- 16 % reduction in volume, two thirds (69 ± 14 %) of which is due to fragmentation and the remainder (31 ± 11 %) is due to basal melting.

1 Introduction

Iceberg calving accounts for roughly half of all ice loss from Antarctica (Depoorter et al., 2013; Rignot et al., 2013). At any time, about 50-90 large icebergs are tracked in the Southern Ocean containing 7 000 to 17 000 km^3 of ice in total (Tournadre et al., 2015). For maritime operators it is essential to know the location of icebergs in order to reduce the risk of collision (Bigg et al., 2018; Eik and Gudmestad, 2010). The thickness of an iceberg determines if and where it will ground on the seabed, which has implications for maritime operations as well as for marine geophysics. Iceberg thickness also influences a wide range of physical and biological interactions with the Antarctic environment. Grounded icebergs can, for example, alter the local ocean circulation (Grosfeld et al., 2001; Robinson and Williams, 2012), melting of the adjacent ice shelves (Robinson and Williams, 2012), and prevent local sea ice from breaking up (Nøst and Østerhus, 2013; Remy et al., 2008). This, in turn, can impact the local primary production (Arrigo et al., 2002; Remy et al., 2008) and pose an obstacle to penguin colonies on their way to their feeding grounds (Kooyman et al., 2007). Temporarily grounded icebergs leave plough marks on the sea floor which can be an important geological record (Wise et al., 2017), but also impact on marine benthic communities (Barnes, 2017; Gutt, 2001). Therefore, iceberg thickness is an important parameter. Changes in iceberg thickness are also important, because they control the quantity of cold fresh water and terrigenous nutrients released into the ocean as icebergs melt (Gladstone et al., 2001; Silva et al., 2006). The release of relatively cold fresh water facilitates sea ice growth (Bintanja et al., 2015; Merino et al., 2016), immediately lowers the sea surface temperature (Merino et al., 2016), and has been found to even influence ocean water down to 1500 m depth (Helly et al., 2011) as well as lead to upwelling of deep ocean properties (Jenkins, 1999). In terms of nutrients, icebergs have shown to be the main source of iron in the Southern Ocean (Laufkötter et al., 2018; Raiswell et al., 2016; Wu and Hou, 2017) and therefore foster primary production in the proximity of icebergs (Biddle et al., 2015; Duprat et al., 2016; Helly et al., 2011), which in turn increases the abundance of krill and seabirds (Joiris, 2018; Smith et al., 2007) around icebergs. Furthermore, a range of studies have demonstrated that including more realistic iceberg distributions, trajectories and volumes in climate models leads to a redistribution of fresh water and heat flux, which agrees better with observations than models that only include small icebergs or that treat iceberg discharge as coastal runoff (Jongma et al., 2009; Martin and Adcroft, 2010; Rackow et al., 2013; Schloesser et al., 2019). To investigate each of these processes and interrelations, knowledge of iceberg thickness and volume and their change over time is required (England et al., 2020; Merino et al., 2016). Moreover, monitoring iceberg melting also presents an opportunity to gain insights into the response of glacial ice to warmer environmental conditions, which may develop at ice shelf barriers in the future (Scambos et al., 2008; Shepherd et al., 2019).

The first detailed studies on iceberg melting were performed in the 1970's and 1980's, and were mainly based on laboratory experiments or ship-based observations (Hamley and Budd, 1986; Huppert and Josberger, 1980; Neshyba and Josberger,

1980; Russell-Head, 1980). These studies found that iceberg melting, to first order, is proportional to the water temperature and that for large icebergs breakage dominates over melting ~~for large icebergs~~. More recently, for example Silva et al. (2006) and Jansen et al. (2007) modelled melting of giant icebergs and the associated fresh water fluxes. The latter found that melting does not only depend on ocean temperature, but also on iceberg drift speed and the surrounding ocean currents. Scambos et al. (2008) installed a range of measurement tools including a GPS receiver, a pre-marked accumulation mast and buried bamboo poles observed with a camera on a large Antarctic iceberg to monitor melting. They differentiate between three kinds of mass loss: rift calving, edge wasting and rapid disintegration. While rift calving can occur at any time within the iceberg life cycle along pre-existing fractures, edge wasting is only observed outside the sea ice edge. Rapid disintegration is caused by surface melting and the formation of surface lakes.

The advent of satellite remote sensing greatly increased our capability to study icebergs. A wide range of studies have employed repeat satellite imagery to track changes in iceberg area (Bouhier et al., 2018; Budge and Long, 2018; Han et al., 2019; Li et al., 2018; Mazur et al., 2019; Scambos et al., 2008). The most common approach to measure iceberg thickness is using satellite altimeter measurements of their freeboard, which began in the late 1980's (McIntyre and Cudlip, 1987). Since then, a range of studies have employed laser and radar altimetry to study freeboard change: Jansen et al. (2007) studied the A-38B iceberg in the Weddell and Scotia Sea with a combination of laser and radar altimetry, and Scambos et al. (2008) also included three Ice, Cloud and land Elevation Satellite (ICESat) overpasses over the A22A iceberg to derive its thickness change. Both studies make use of satellite imagery to ~~geolocate~~ colocate the altimetry tracks and to compare similar areas in terms of freeboard change. In contrast, Tournadre et al. (2015) employed altimetry measurements from Envisat, Jason1 and Jason2 to analyse freeboard change of the C19A iceberg without any ~~geolocation~~colocation. Bouhier et al. (2018) analysed thickness changes of the B17A and C19A icebergs in open water using altimetry data without ~~geolocation~~colocation.~~,~~ Li et al. (2018) calculated freeboard change of the C28A and C28B icebergs for two years at the intersections of CryoSat-2 overpasses, and Han et al. (2019) also used intersecting CryoSat-2 tracks to calculate freeboard change of the A68 iceberg in the Weddell Sea. When thickness and area changes are combined, it is possible to detect changes in iceberg volume (Bouhier et al., 2018; Han et al., 2019; Tournadre et al., 2015). However, studies to date have been limited to selected icebergs, have focussed on the Weddell Sea, and have employed a variety of approaches to account for the irregular sampling of altimetry tracks including manual ~~geolocation~~ colocation of entire tracks relative to the initial surface (Jansen et al., 2007), ~~geolocation~~ colocation of intersecting tracks (Han et al., 2019; Li et al., 2018), and with no ~~geolocation~~ colocation at all (Bouhier et al., 2018; Tournadre et al., 2015). ~~More recently,~~Also satellite stereo photogrammetry (Enderlin and Hamilton, 2014; Sulak et al., 2017) and interferometry (Dammann et al., 2019) have been employed to measure iceberg thickness and volume as an alternative approach, though in our experience both methods are labour intensive.

In this study, we quantify changes in the area, freeboard, thickness and volume of the B30 iceberg, which has been adrift in the Southern Ocean since it calved from the Thwaites Glacier 8.5 years ago (Budge and Long, 2018; Fig. 1). The long life-cycle and large drift of the B30 iceberg results in a relatively high number of observations, enabling a detailed study of its evolution. This is one of the first studies to investigate iceberg thinning in the Southern Ocean around Marie Byrd Land. ~~and w~~We also assess the agreement between estimates of freeboard change determined relative to the average initial surface and using precise c~~ge~~olocation with the aid of near-coincident satellite imagery. Moreover, we develop a methodology to account for snowfall and the evolutions of snow and ice density and examine the influence of snow on the iceberg thickness calculation. The next chapter introduces the remote sensing data used in this study and explains our methodology; the third chapter presents our results on iceberg area, freeboard, thickness and volume change in turn and discusses our findings. We close with conclusions and a brief outlook in chapter four.

2 Data and m~~M~~ethods

To chart the iceberg area change over time we delineate its extent in a sequence of Moderate Resolution Imaging Spectroradiometer (MODIS) optical satellite imagery and Sentinel 1 synthetic aperture radar (SAR) satellite imagery. We then use CryoSat-2 satellite radar altimetry to determine changes in the iceberg freeboard and thickness, assuming that it is floating in hydrostatic equilibrium, and making use of the iceberg orientation relative to its initial position using near-coincident satellite imagery on some occasions. We account for snow accumulation and model variations in snow and ice density when converting iceberg freeboard to thickness. Finally, we combine both data sets to estimate the iceberg's volume change over time.

2.1 Iceberg location

We use daily archived iceberg positions from the Antarctic Iceberg Tracking (AIT) database version 3.0 provided by the Brigham Young University (Budge and Long, 2018) as a baseline estimate of the B30 iceberg location since it calved in 2012 (Fig. 1). The AIT database makes use of coarse-resolution passive microwave scatterometer imagery in which icebergs are manually detected and the central position is recorded daily. It includes icebergs longer than 6 km adrift in the Southern Ocean between 1987 and 2019, augmented with estimates of position and the semi minor and major axes lengths of icebergs longer than 18.5 km that are tracked operationally by the U.S. National Ice Center (NIC) using a combination of visible, infrared and SAR imagery.

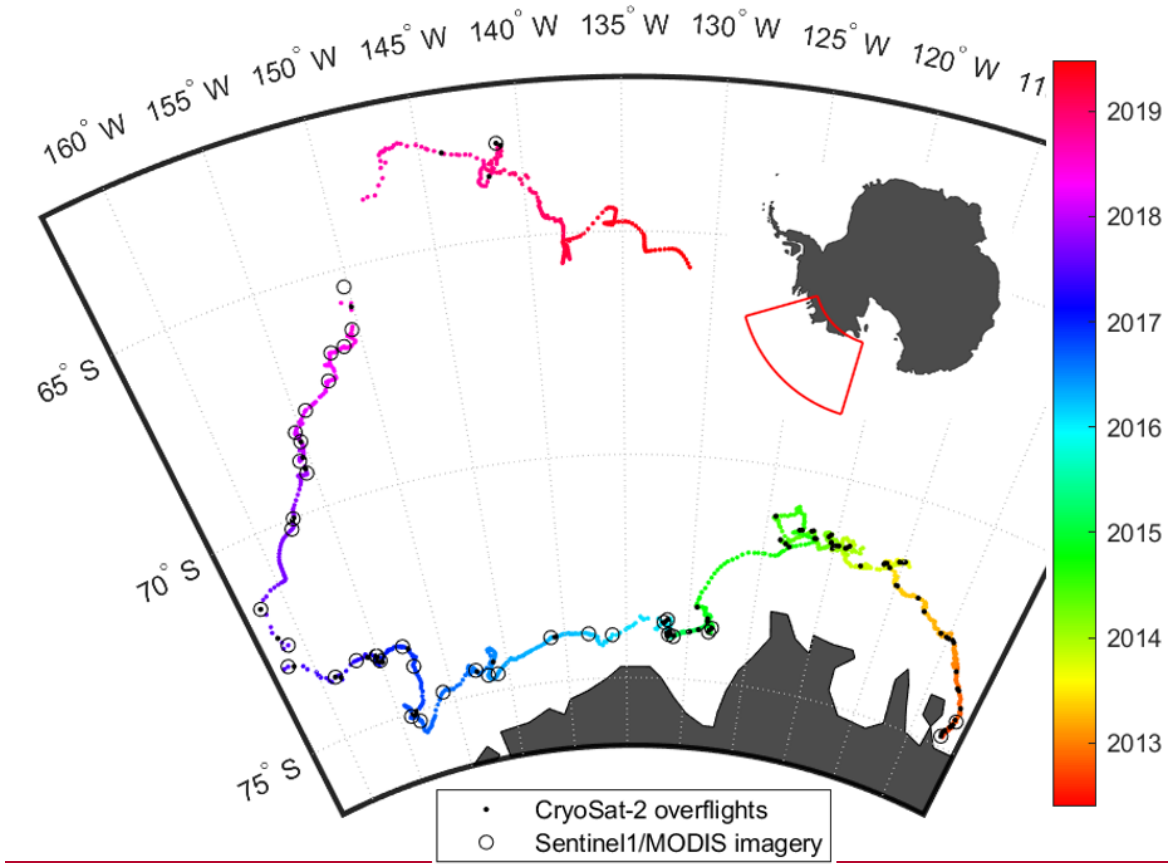
160° W
155° W
150° W
145° W
140° W
135° W
130° W
125° W
120° W
65° S
70° S
75° S
2019
2018
2017
2016
2015
2014
2013
CryoSat-2 overflights
Sentinel1/MODIS imagery

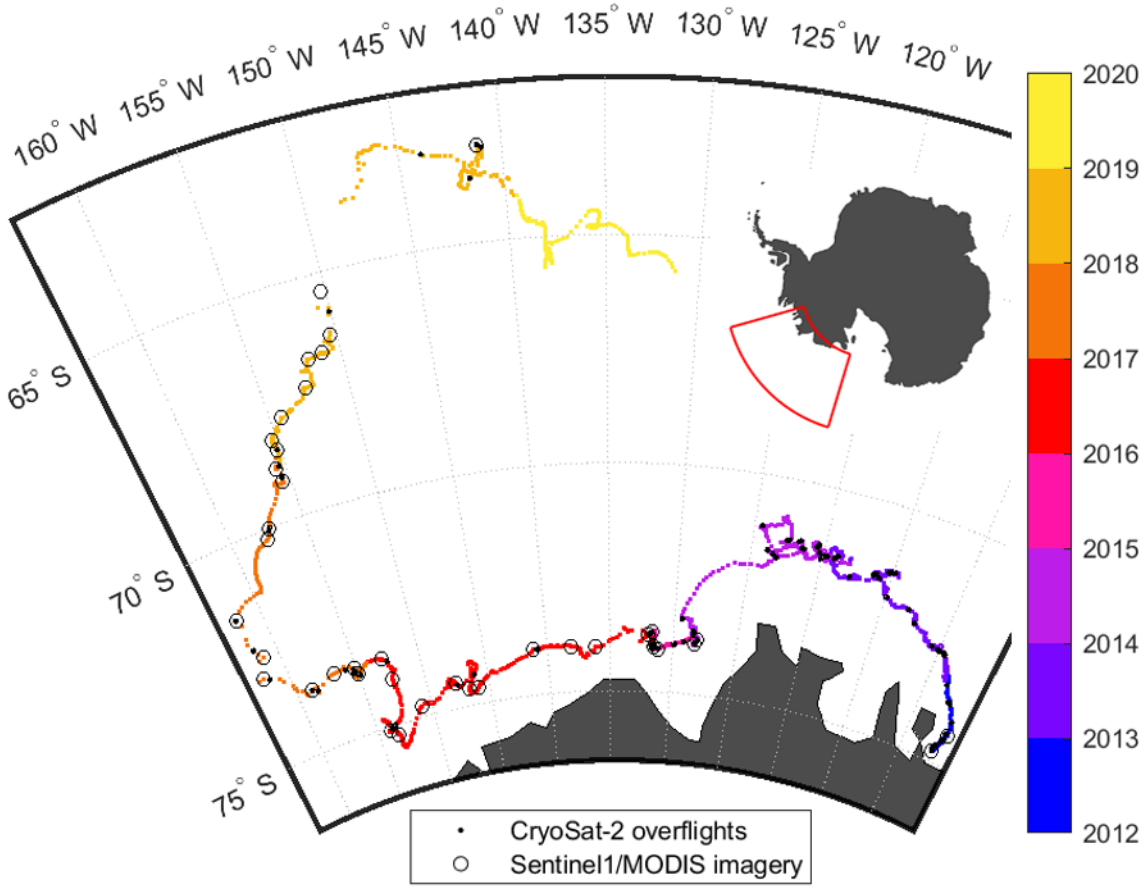

Figure 1: Trajectory of the B30 iceberg as recorded by the Antarctic Iceberg Tracking Database (Budge and Long, 2018): After calving from the Thwaites ice shelf in 2012, it followed the coastal current westwards, started drifting north in 2017 and eventually disintegrated in 2019. Black dots mark the positions where CryoSat-2 overflights over the iceberg are available, circles depict the positions of the MODIS and Sentinel 1 images used in this study

2.2 Initial iceberg shape, size and calving position

To determine the initial shape, size and calving position of B30, we use MODIS images acquired before and after the calving event to identify which section of the Thwaites ice shelf calved to form the iceberg. MODIS is an instrument on the Terra and Aqua satellites by NASA launched on 18th December 1999 and 4th May 2002, respectively. The instrument measures radiance in the visible and infrared range with a spatial resolution of 250 m to 1 km and covers the entire Earth in 1-2 days, though cloud occlusions and the absence of daylight reduce data availability for many applications. For this study we use bands 1 (red), 4 (green) and 3 (blue) of the MODIS Level 1B calibrated radiances at 500 m resolution

(MOD02HKM). As B30 broke off on 24 May 2012 (Budge and Long, 2018) in Antarctic winter, during darkness, the closest useful MODIS imagery is from the preceding autumn and subsequent spring. We use several MODIS images acquired in the subsequent spring after calving to determine the initial shape, as it is difficult to unambiguously distinguish the berg from clouds and sea ice in a single image. The initial perimeter (Figure 2a, 3a) was then shifted and rotated to fit the situation before calving to identify the part of the Thwaites ice shelf that formed B30 (Fig. 4). The initial ~~size~~ area (in plan-view) of the iceberg is 1500 km^2 with a long axis of around 59 km (Budge and Long, 2018).

2.3 Iceberg area

We employ three approaches to estimate the plan-view iceberg area; (i) manual delineation in sequential satellite imagery scenes, (ii) using measurements of the semi-major and semi-minor axes provided by the NIC and assuming an elliptical shape and (iii) using measurements of their arc lengths recorded in satellite altimetry and assuming a circular shape. While manual delineation provides the most consistent and accurate area estimate, the axes and arc length approaches are much simpler to implement and can be fully automated.

Our main approach to determine iceberg area is manual delineation using a sequence of 32 Sentinel-1 SAR and 8 MODIS optical imagery. Sentinel 1A and 1B are companion imaging radar satellites launched by the European Space Agency on 3rd April 2014 and 25th April 2016, respectively. Together, they provide repeat sampling of the Earth's surface every 6 days. For this study, we use Level 1 Ground Range Detected (GRD) data. Depending on availability, both interferometric wide (IW) and extra wide (EW) swath mode are used, but over the open ocean only EW data are acquired. We employ the Sentinel Application Platform (SNAP) toolbox to apply the orbital and radiometric corrections. The SAR images were multi-looked with a factor of six to reduce speckle and computation time, leading to a spatial resolution of 240 m. Finally, a terrain correction was applied using the GETASSE30 (Global Earth Topography And Sea Surface Elevation at 30 arc second resolution) digital elevation model. The resulting backscatter values are scaled between their 5th and 95th percentiles ~~and translated to a polar stereographic projection~~. The MODIS optical imagery were required prior to the launch of Sentinel-1A in 2014.

To chart changes in the iceberg area over time, we delimit its outline as a polygon in each subsequent image (Fig. 2). When the iceberg is drifting in open water its outline can be detected automatically using boundary detection techniques (e.g. using matlab's bwboundaries function). However, in the presence of sea ice the iceberg could not be separated using this approach, and so we instead delimit its outline manually on such occasions. If parts of the iceberg are covered by clouds, we again use multiple MODIS images together, so that different parts of the iceberg are obscured by clouds in each image (e.g. Fig 3l). Also sea ice frozen to the iceberg is easier to distinguish from its colour and texture, when several images are used together (e.g. Fig 3b, c). To estimate the accuracy of our delineations we shrink and expand the polygons by one pixel

(500 m for MODIS images and 240 m for multi-looked Sentinel 1 images) and calculate the resulting difference in area.

160 This gives a mean relative difference of 3.6 ± 0.9 %.

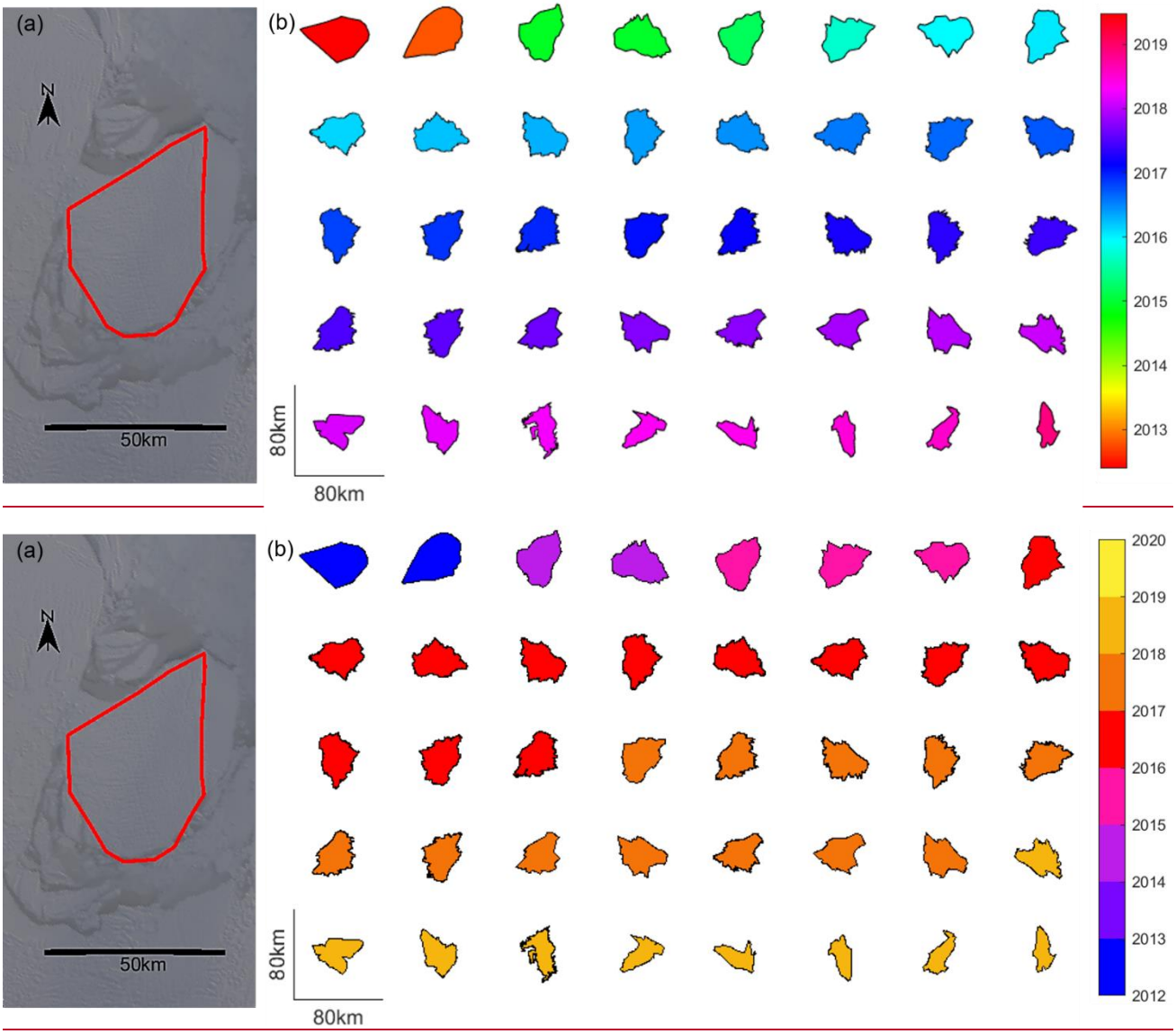

Figure 2: Outlines of the B30 iceberg derived from satellite imagery. a) Initial shape (red polygon) of the B30 iceberg determined from MODIS images after calving; the background is a MODIS image on 11 September 2012. b) Polygon outlines derived from
165 **further MODIS and Sentinel 1 imagery plotted in polar stereographic projection and used to calculate area change of the B30 iceberg.**

Our second method of estimating the iceberg area is based on 228 measurements of the semi-major and semi-minor axes lengths. Although iceberg area is most accurately calculated from delineation of their full perimeter in satellite images, the downside of this approach is that it requires a high degree of time-consuming manual interaction and clear imagery. This also makes it less reproducible and subject to individual judgement. We estimate the size of an ellipse calculated from the semi major and minor axis provided by the NIC and compare this with our imagery-based iceberg area calculations. The NIC operationally tracks icebergs longer than 18.5 km using a combination of visible, infrared and SAR imagery. Observations are made weekly but especially in the early days longer data gaps exist and not every estimate of semi axes length is based on a new manual observation, but some are just duplicated from the previous observation. Their estimates of semi axes lengths are also rounded to nautical miles (1.852 km), leading to a stepwise evolution of iceberg area with only 8 different estimates. We base our trend estimate and analysis solely on these 8 estimates, because we are confident that these are unique observations. The uncertainty of this approach is governed by the assumption of an elliptical iceberg shape and the irregular, rounded updates.

Our third and final method of estimating the iceberg area is to make use of 106 CryoSat-2 satellite altimeter overpasses, which are also used to calculate the iceberg's thickness. ~~that~~We record the arc lengths of the iceberg sampled by these tracks and estimate iceberg area by assuming the iceberg has a circular shape. Depending on the position and relative orientation of the iceberg with respect to each overpass, CryoSat-2 will occasionally sample the long axis, but more often a shorter corner. This leads to ~~significant~~ considerable variations in the area estimates, and in general an underestimation. We employ a ten-point moving mean along time to reduce the variability. The principal uncertainty of this approach is because one-dimensional arc lengths cannot reliably represent a two-dimensional area especially when the shape is evolving and if it is unknown which part of the shape was sampled.

2.4 Iceberg orientation

To track the iceberg shape and rotation in later images relative to its initial orientation, we record the iceberg's orientation in all satellite images that are near-coincident in time with CryoSat-2 overflights (Fig. 3) ~~and therefore used for geolocation~~. To orientate the iceberg, we manually ~~click~~ identify the coordinates of one corner of the initial iceberg polygon outline at the time of each new overpass and adjust the rotation angle to align (colocate) all images to a common orientation (Fig. ~~3~~7a-l). This allows us to transform the iceberg coordinates at the time of each image acquisition relative to the equivalent position at the time just before it calved.

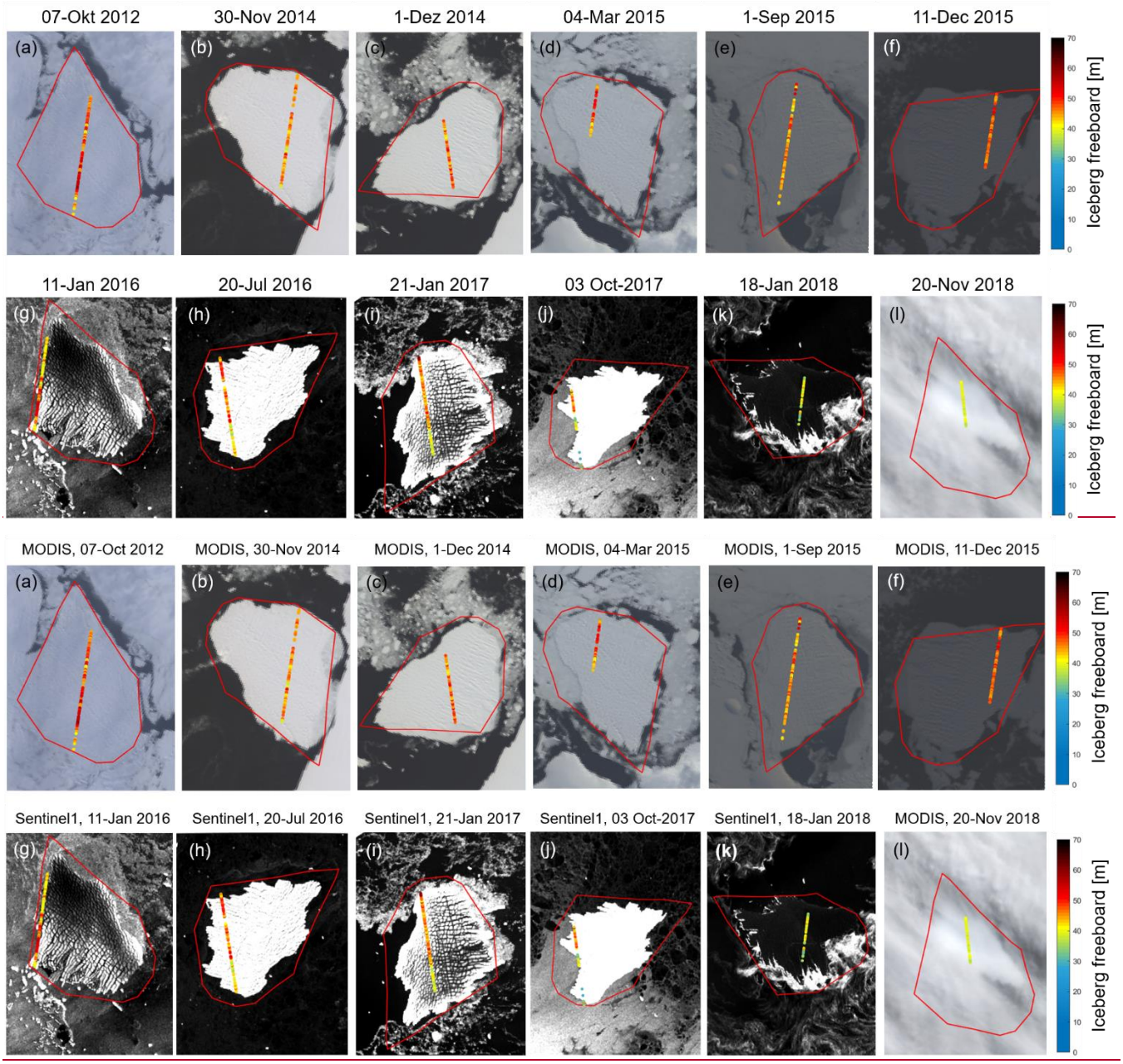

Figure 3: Satellite imagery with near-coincident CryoSat-2 tracks of iceberg freeboard and the manually transformed initial polygon shape plotted on top. The initial polygons are used to determine the relative position of each new overpass.

2.5 Initial iceberg freeboard

We use CryoSat-2 satellite altimetry to determine freeboard and thickness of the B30 iceberg. CryoSat-2 is a satellite radar altimeter that employs SAR processing to achieve along track resolution of 250 m. It was launched by the European Space Agency on 8 April 2010 in a 369-day repeat period with a 30-day sub cycle. We use Level 1B baseline C ~~-~~data from the CryoSat-2 Science server and apply the Centre for Polar Observation and Modelling sea ice processing system (Tilling et al., 2018) to deduce surface height. For consistency, a common threshold retracker is applied to measurements acquired in both SAR and SAR interferometric mode and over all surface types. Using Level 1B data is important, because the Level 2 products are generated using different retrackers and using different biases for different modes and surface types, and so the signals acquired during different parts of the iceberg trajectory are not comparable. Iceberg freeboard is calculated by subtracting the adjacent mean sea surface height from the iceberg surface height.

Although satellite altimeters only sample icebergs along 1-dimensional profiles beneath their ground track while they are drifting, it is possible to build up a detailed 2-dimensional picture of their surface over time prior to calving while their movement is relatively modest. To map the initial freeboard height of B30, we combine all CryoSat-2 tracks recorded within almost 5 months (1 January 2012 to 24 May 2012) before it calved (Fig. 4a). The Thwaites Glacier ice shelf flows at 3.9 km per year on average (Mouginot et al., 2019), and so we adjust earlier tracks to account for this movement. Because the Thwaites ice shelf has a particularly rugged and crevassed surface topography, the point-of-closest-approach (POCA) varies. To make different overpasses more comparable, we remove outliers by deleting freeboard heights greater than 60 m or below 20 m freeboard (Tournadre et al., 2015), and crevasses by deleting freeboard heights falling either below the median minus one standard deviation or below the 5-point moving mean minus the 5-point moving standard deviation. The mean initial unfiltered iceberg freeboard is 45.5 m above the adjacent sea level with a wide spread of 8.1 m standard deviation. When crevasses are excluded, the mean freeboard is 49.0 m with a much lower standard deviation of 4.6 m. Because the resulting freeboard measurements are still quite sparse, we average them within 5 km grid cells to obtain a continuous reference surface (Fig. 4). The number and standard deviation of the gridded freeboards give an indication of the variance within each grid cell. The mean standard deviation within each grid cell is 3.3 m, the standard deviation across different grid cells is 3.1 m and the overall standard deviation of all heights within the polygon is 4.6 m. We compare the gridded initial freeboard to measurements from the first CryoSat overpass when the iceberg is adrift, acquired shortly after calving, to check they are consistent, and find a mean difference of -0.4 m. As this value is considerably~~significantly~~ lower than the iceberg freeboard variability, we conclude that the ice shelf was floating freely prior to calving also, and that the gridded heights are representative of the initial freeboard.

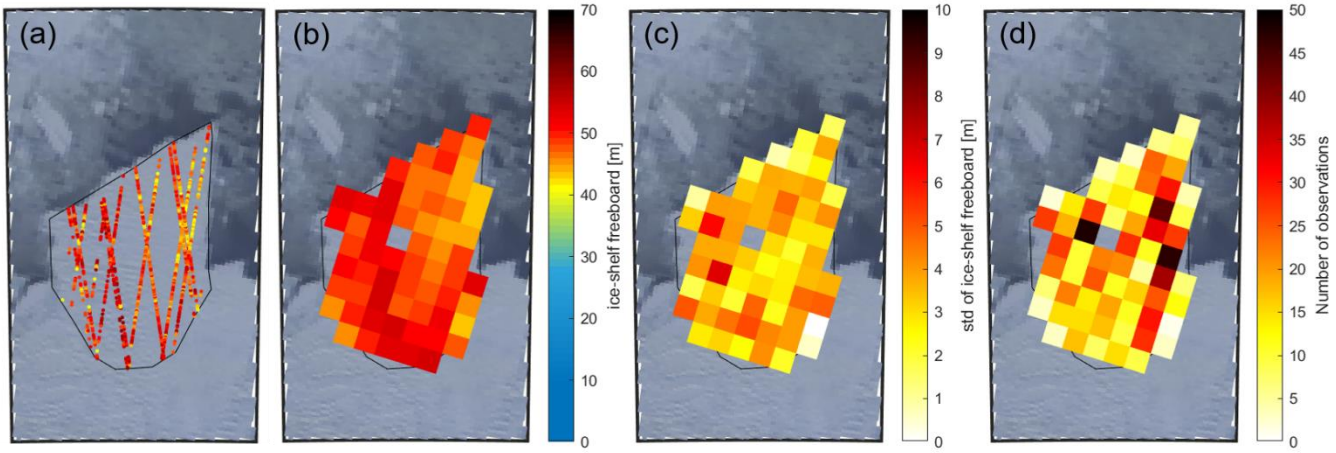

Figure 4: Initial freeboard heights of the B30 iceberg overlain on a MODIS image on 19 March 2012 (before calving). a) Filtered CryoSat-2 measurements of 145 days before calving, b) Gridded CryoSat-2 data, c) Standard deviation of the gridding, d) Number of measurements per grid cell

2.6 Iceberg freeboard change

When icebergs are adrift, their motion is sufficiently large to mean that they are only sampled in 1-dimensional profiles along satellite altimeter ground tracks (Fig. 3). We extract surface heights over the B30 iceberg when it is adrift (e.g. Fig. 5) using the position from the AIT database as an initial estimate of its location. However, because the AIT positions and timings are approximate and the iceberg has a significant extent, we investigate all CryoSat-2 ground tracks that pass within 1-degree latitude and 2-degrees longitude of the database position. We automatically extract measurements sampling the iceberg with the following steps: Track segments are truncated to exclude altimeter echoes from targets where the first or last freeboard height is more than 3 m, to exclude measurements from the nearby continent, and we also exclude tracks that do not contain freeboard measurement between 20 and 60 m, to ensure that they sample the iceberg. We consider all freeboard heights between the first and last echo falling in the range 20 to 60 m as potential iceberg measurements (Tournadre et al., 2015). To avoid including adjacent icebergs or berg fragments, we exclude segments with more than 10 measurements of ocean or sea ice, identified as surface heights in the range -3 to +3 m, between potential iceberg measurements. We also remove crevasses and other rugged features using the same editing steps applied to determine the surface height prior to calving. As a final check, we calculate the distance of these remaining heights to the AIT database location, and discard measurements that are further away than half the iceberg length (28 km) to ensure we are tracking B30.

We apply two different techniques to calculate changes in the iceberg freeboard. For 12 tracks we are able to calculate precise changes in freeboard with spatial definition by making use of near-coincident satellite imagery to account for the rotation and translation of the iceberg relative to its initial position prior to calving and consider the estimated movement between the time of the nearest satellite image and altimeter acquisitions. At 94 other times, we compute the freeboard height change as the difference of mean freeboard from each new overpass relative to the initial mean surface height. While these observations are of poorer certainty, they provide denser temporal sampling and fill gaps between the ~~geolocated~~ colocated measurements. The first "co-location" method assigns both the initial heights and the new measurements to their closest 5 km grid cell and averages them to ensure that the same locations are compared. We account for the iceberg drift between the times of the satellite acquisitions, allowing a maximum separation of 72 hours (though most overpasses are separated by less than 24 hours). If the image is from a different date than the CryoSat track, we correct the distance travelled based on the daily iceberg locations from the AIT database. In any case, we account for the drift in our uncertainty estimate~~. We~~ performing a Monte Carlo simulation with 1000 slightly differently collocated samples per track. These are normally distributed around our estimated translation and rotation with a standard deviation of 15° per day and a drift speed of 3 km per day (Scambos et al., 2008) scaled by the respective time separation. We then calculate the freeboard difference for each of the 1000 slightly differently collocated tracks and use the resulting standard deviation of freeboard change from these samples as the uncertainty of our colocation. ~~assume a translational uncertainty of 3 km per day (Scambos et al., 2008) and a rotational uncertainty of 15° per day. Both are scaled by the time difference between the image and the CryoSat overpass. We then perform a Monte Carlo simulation to assess how these positional uncertainties translate to uncertainty in freeboard change.~~ This is combined with the standard deviation of the gridded CryoSat-2 freeboard data (of the new track and of the reference) to yield a conservative~~n~~ uncertainty estimate for the ~~geolocated~~ colocated tracks. The second method ignores the relative position and orientation of the iceberg at the time of the altimeter overpasses, and simply compares the mean freeboard along each new track to the mean surface height before calving. Although this method is easiest, since it does not rely on additional image data to locate the track, it cannot account for potential spatial variations in the iceberg freeboard. Because of this, we restrict the new overpasses to those including at least 20 measurements, as tracks sampling only the edges of an iceberg tend to be inaccurate. As uncertainty estimate we combine the standard deviation of each new overpass with the standard deviation of the initial height. As a first check to see if the mean freeboard from a single overpass can be compared to the mean initial height, we calculate the mean height for each of the 15 tracks over the pre-calved iceberg (Fig. 4a) and find a standard deviation of 2.8 m compared to the mean initial height of 49.0 ± 4.6 m.

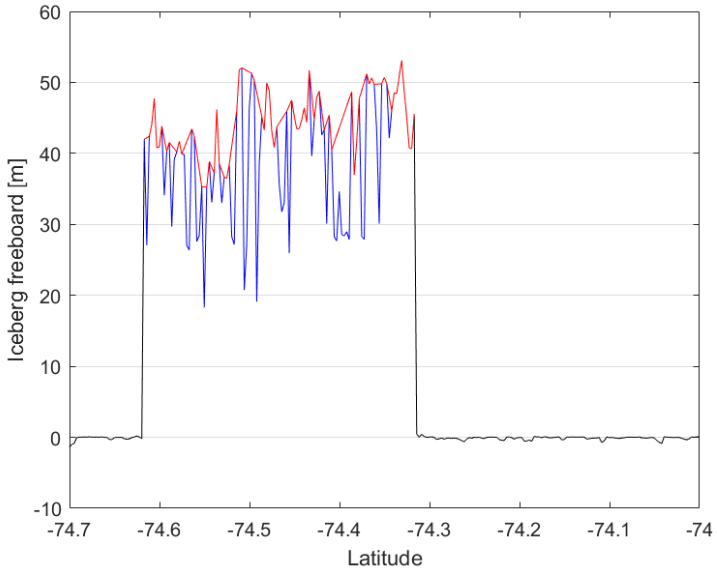

Figure 5: Example of CryoSat-2 freeboard measurements along one track. The blue line shows which heights were identified as iceberg and the red line shows the remaining heights after filtering out crevasses.

2.7 Iceberg thickness

We compute iceberg thickness H (freeboard plus draft) from our estimates of iceberg freeboard heights h_{fb} assuming hydrostatic equilibrium and that CryoSat-2 does not penetrate through the snow layer (Eq. 1; Moon et al., 2018). Besides these freeboard heights, iceberg thickness also depends on column-average densities of sea-water- ρ_w , ice ρ_i and snow ρ_s as well as snow depth h_s. Including a snow layer in this equation is important, because the snow layer adds to the observed freeboard and disguises a part of the ice freeboard change. On the other hand the additional load of the snow layer pushes the iceberg downwards. Both effects are taken into consideration. We assume sea-water density to be 1024 kg m^{-3} (Fichefet and Morales Maqueda, 1999) and set its uncertainty to 2 kg m^{-3}. Due to the long life cycle of the B30 iceberg of 6.5 years and the changing environmental conditions it experiences during this time, we allow the ice and snow densities to evolve with time. Snow depth is also time-varying, and estimates of this and of snow and ice density are introduced successively.

$$H = \frac{\rho_w}{\rho_w - \rho_i} h_{\mathrm{fb}} - \frac{(\rho_w - \rho_s)}{\rho_w - \rho_i} h_s \quad (1)$$

To estimate the thickness of the snow layer, we download hourly ERA5 Reanalysis snowfall, snowmelt and snow evaporation data (Copernicus Climate Change Service, 2018), accumulate it daily and interpolate it in space and time to the iceberg's trajectory. Snowmelt and snow evaporation are subtracted from the snowfall to retrieve the additional snow

accumulation since calving. However, this snow estimate does not account for snow being blown off the iceberg or onto the iceberg from the continent. To convert snow water equivalent (SWE) to snow depth, we need to know snow density. Snow density is time variable because snow compacts gradually during the iceberg's life time of several years as a function of snow depth h_s [m], the mean air temperature T [°C] and the mean wind speed v [$\mathrm{m \cdot s^{-1}}$] (Eq. 2; International Organization for Standardization, 1998). We use hourly ERA5 Reanalysis 2 m air temperature data and calculate wind speed from the ERA5 Reanalysis 10 m eastwards and northwards wind components (Copernicus Climate Change Service, 2018). Both are interpolated to the iceberg's trajectory and averaged since the day of calving. Because snow density depends on snow depth and snow depth depends on snow density, we calculate both iteratively starting with a snow density of 300 kg m^{-3}. We set the uncertainty in snow density to 50 kg m^{-3} (Kurtz and Markus, 2012) and the uncertainty in snow depth to 20%.

$$\rho_s = \left(90 + 130 \cdot \sqrt{h_s}\right) \cdot \left(1.5 + 0.17 \cdot \sqrt[3]{T}\right) \cdot \left(1 + 0.1 \cdot \sqrt{v}\right) \quad (2)$$

To calculate the iceberg's ice density profile we follow the approach by Tournadre et al. (2015), and determine two parameters V and R to fit the surface density and the depths of the critical density levels (550 kg m^{-3} and 830 kg m^{-3}) of the Thwaites Ice Shelf, from which it calved, as given in Ligtenberg et al. (2011; Eq. 3). ρ_g is the density of pure glacial ice (915 kg m^{-3}). Since the mean ice density depends on ice thickness and ice thickness depends on the mean ice density, we iterate over both equations. We also account for ice density changes over the iceberg's life cycle by calculating new mean densities as the iceberg thins. This incrementally reduces the average ice density as the densest ice is melted at the bottom. As ice density uncertainty we take 10 kg m^{-3}.

$$\rho_i = \frac{1}{H} \int_0^H (\rho_g - V \cdot e^{R \cdot z})\, dz \quad (3)$$

3 Results and dDiscussion

We first assess changes in the B30 iceberg area using boundaries mapped from satellite imagery, and we compare the observed trend to ~~more approximate~~less accurate estimates derived from arc-lengths and semi-major axes. Next, we determine the change in iceberg freeboard and we assess the impact of employing precise ~~geolocation~~ colocation using near-coincident satellite imagery. Iceberg thickness changes are then computed from freeboard changes using time-varying estimates of snow accumulation and snow and ice densities derived from atmospheric reanalyses. Finally, iceberg area and thickness changes are combined to derive the change in volume and mass.

3.1 Iceberg aArea cChange

When the B30 iceberg first calved in May 2012, it was 1500 ± 60 km^2 large. Over the following 6.5 years it lost 1075 ± 66 km^2 of its extent, which corresponds to a 72 ± 11 % reduction at an average rate of 149 ± 5 km^2 per year (Fig. 6). However, because delineating iceberg outlines requires a high degree of time-consuming manual interaction, we also evaluate the efficacy of two alternative methods based on measurements of their orthogonal (semi-major and semi-minor) axes by the NIC and on arc lengths recorded in satellite altimetry which are considerably less laborious. Although these approaches also yield progressive reductions in area (Fig. 6), they exhibit significant positive (138 km^2, 14%) and negative (-426 km^2, 45%) biases, respectively, due to under-sampling of the iceberg geometry and the necessary approximation of a regular shape (ellipses and circles, respectively). While an ellipse overestimates the area compared to most shapes with the same axes, arc lengths yield an underestimate because corners are sampled more often than the major axis. One idea for improvement would be to use the maximum or to filter out tracks that only sample one corner, but the main problem remains that a one-dimensional length measurement cannot be translated into a reasonable area estimate without knowing the iceberg shape, which changes over time. Nevertheless, both the orthogonal axes and arc-length approaches yield area estimates that are reasonably well correlated ($r>0.90$) with those determined from our manual delineation. Area trends are overestimated by 16% and underestimated by 48%, respectively. While manual delineation provides the most consistent and most accurate area estimate, tracking iceberg axes or arc lengths yields area and area change estimates that are within 48% and is considerably less time consuming.

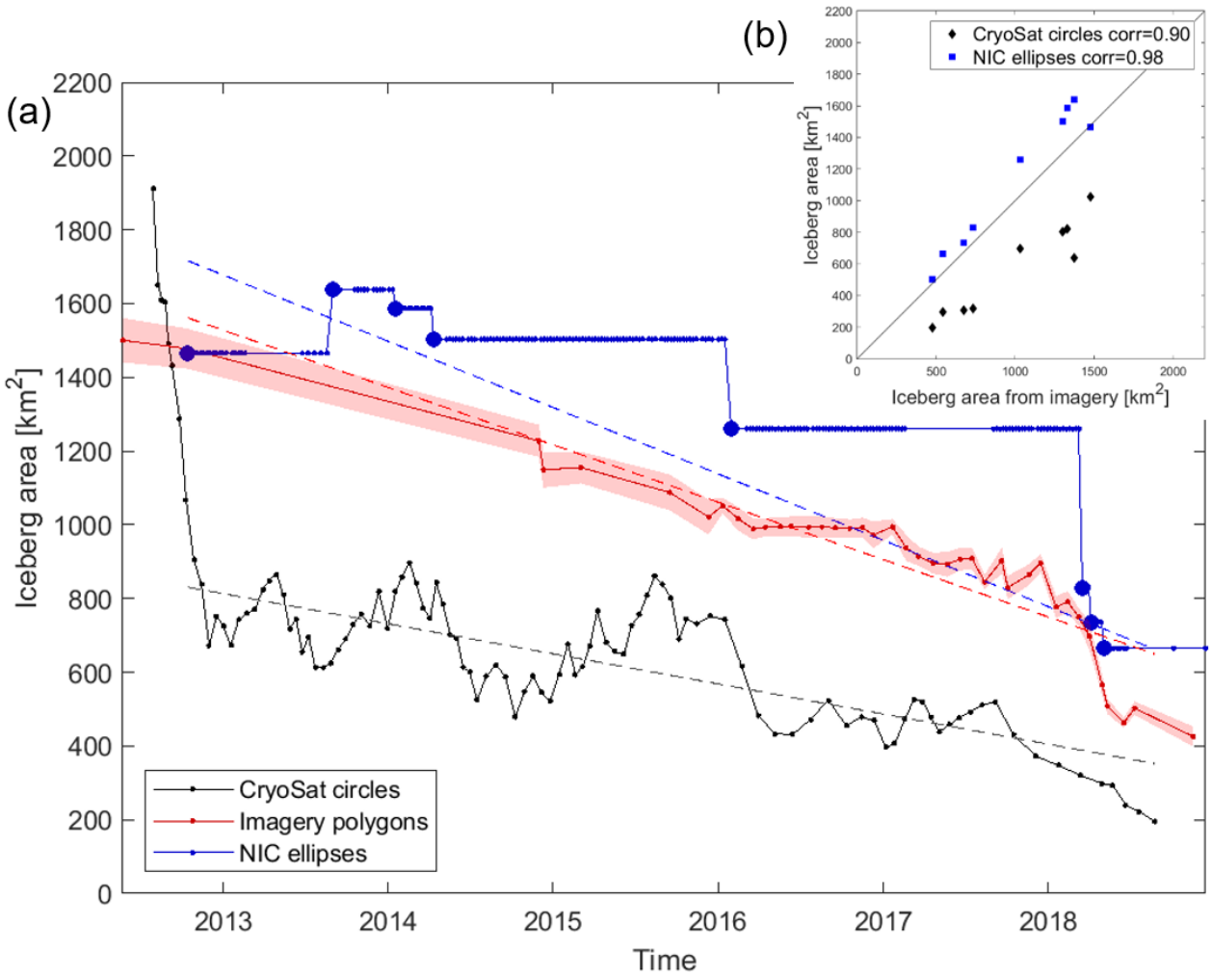

Figure 6: Area change of the B30 iceberg from polygons delineated in satellite imagery with their uncertainty (red) and approximations using orthogonal axes provided by the National Ice Center (NIC) assuming an elliptical shape (blue) or using the arc lengths of CryoSat-2 overflights assuming a circular shape (black) over time (a) and as scatter plot (b). To fit the NIC trend line in (a) we only use unique values of orthogonal axes length (thick blue dots). These also define the dates of comparison in (b).

The rate of iceberg area loss from B30 was approximately constant until 2018, after which time it started to lose larger sections ~~and~~ more rapidly. Although its area has reduced steadily over time, it is less obvious which sections have been lost during individual calving events. However, by aligning the initial polygon to each subsequent image (Fig. 3) it is possible to identify when and where changes occur. The iceberg shape already appears altered on 30th November 2014, after bumping into the adjacent ice shelf which likely caused the first chunks to break off. B30 continued to lose smaller

sections along its edges over the next year – either through melting at the sides or smaller wastings – when it was drifting along the coastal current. In 2018, bigger sections are lost more rapidly, as the iceberg is drifting northwards in open water. Rift calving can occur at any time within an iceberg life cycle along pre-existing fractures (Scambos et al., 2008), while edge wasting is typically only observed when icebergs are travelling outside the sea ice pack. B30 was heavily crevassed prior to calving (e.g. visible in Fig. 3g and i), and so even the smaller wastings along its edges could reflect rift calving events rather than edge wastings. Another possibility is the 'footloose mechanism' (Wagner et al., 2014), which can become a main driver of iceberg decay in warm waters when wave erosion at the waterline forms a sub-surface foot, creating a buoyancy stress that can lead to calving. Although it is not possible to investigate the effects of wave erosion using satellite data, the effect could in principle have caused the larger break-ups that occurred in 2018.

3.2 Iceberg ~~f~~Freeboard ~~c~~Change

To assess the change in freeboard over the survey period, we compare differences between the new overpasses and the initial heights in space and time (Fig. 7). For the spatial analysis we chart the freeboard difference between each new ~~geolocated~~ colocated overpass (Fig. 3) and the gridded initial height (Fig. 4b) at the same relative iceberg position. This comparison shows that the change in freeboard height across the iceberg is relatively homogenous at each epoch (Fig. 7a-l). We then average these differences per CryoSat-2 track and chart the variation over time alongside the less accurate (but more abundant) estimates determined without ~~geolocation~~ colocation (Fig. 7m). Because the observations without ~~geolocation~~ colocation are relatively imprecise, we apply a 10-point moving mean to the data and we also fit a polynomial of 3rd order (and starting at zero) to model the trend. Overall, the B30 iceberg freeboard has reduced by 9.2 ± 2.2 m during the 6.5 years since it calved.

To assess the importance of ~~geolocation~~colocation, we compare freeboard changes calculated with and without this step (Fig. 7n). The estimates are well correlated (r=0.87) and the root mean square difference is 1.6 m, which is a measure of the improvement in certainty associated with ~~geolocation~~ colocation and equal to the difference in mean uncertainty of ~~geolocated~~ colocated tracks (4.7 m) versus tracks without ~~geolocation~~ colocation (6.3 m). Also, the temporal variation of freeboard changes computed from observations with and without ~~geolocation~~ colocation are in good overall agreement (Figure ~~5a~~7m), and we conclude that for this iceberg we can combine the two and make use of the entire set of CryoSat-2 measurements. This finding should hold for other tabular icebergs where the topographic variability is smaller than the observed thinning. The variability of freeboards computed within each 5 km grid cell and across different grid cells are also of the same order – 3.3 m and 3.1 m, respectively – and this is likely to have reduced the impact of ~~geolocation~~ colocation uncertainties. For other icebergs with more heterogeneous freeboard across the iceberg that are less crevassed

(i.e. with lower freeboard variabilities within the same grid cell), colocation might have a larger impact and more icebergs need to be studied to generalise these findings.

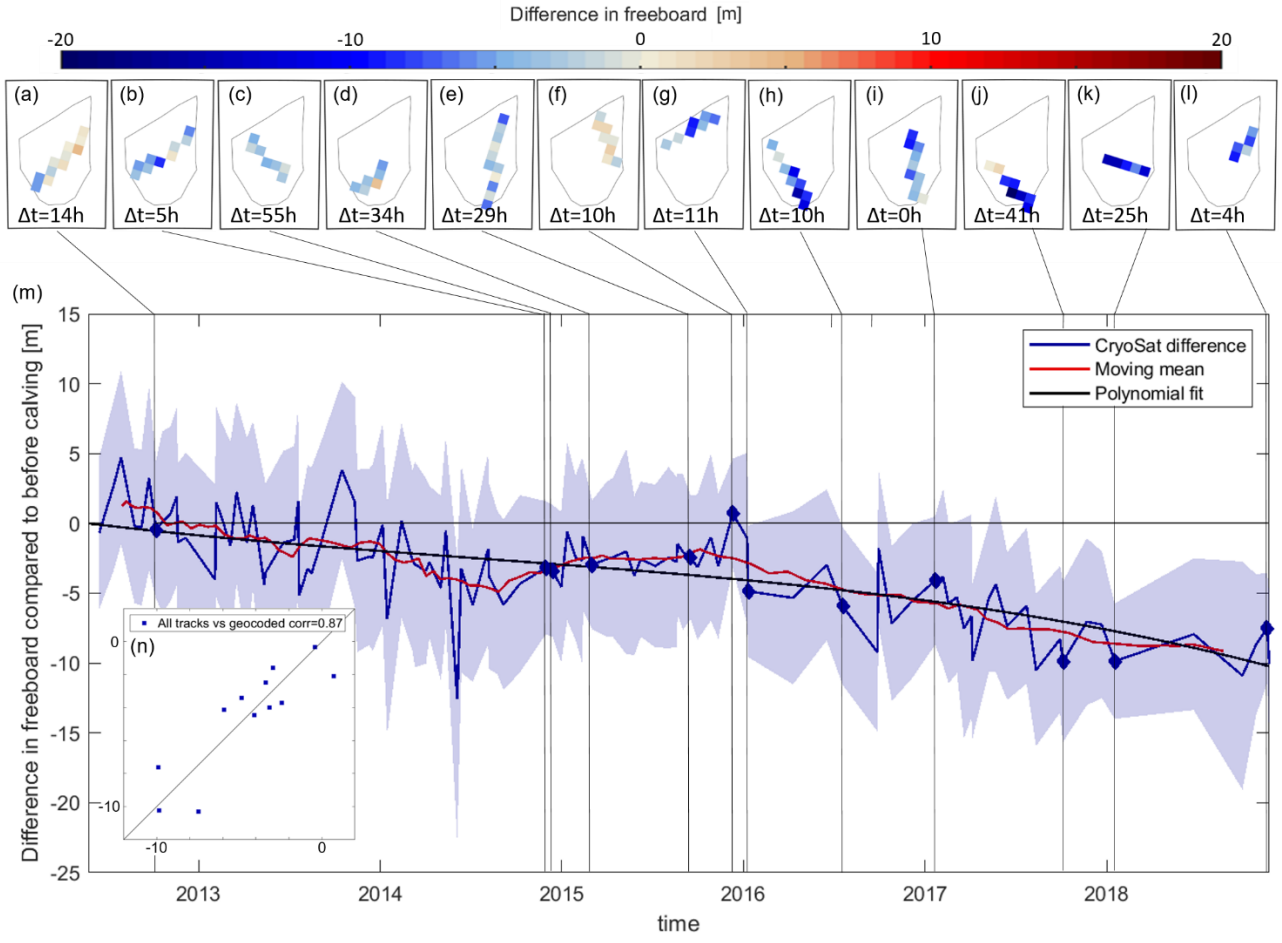

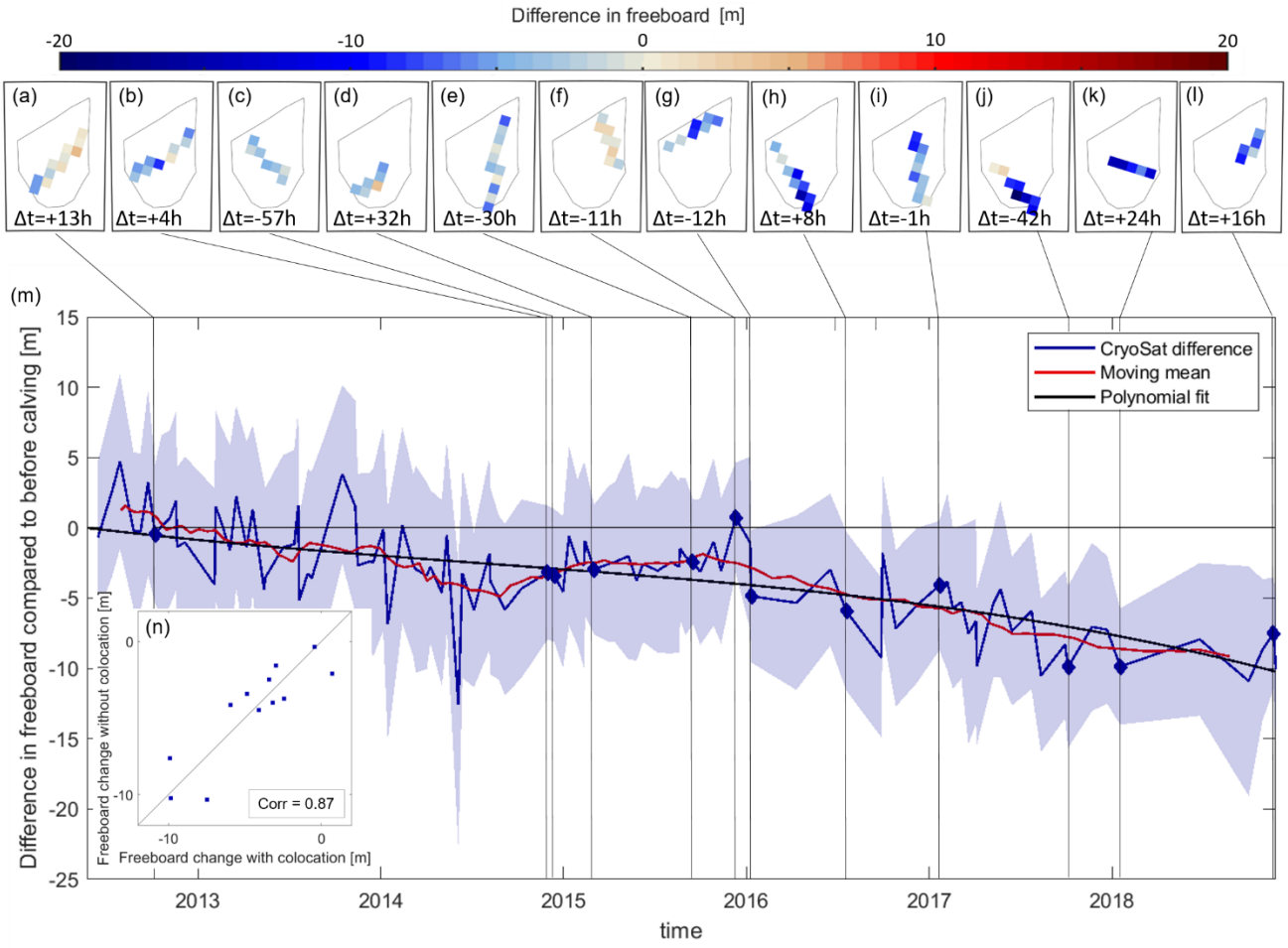

Figure 7: Freeboard change of the B30 iceberg. a-l) Freeboard difference in each grid cell sampled by colocated CryoSat-2 overpasses; the Δt values give the time difference between the CryoSat-2 overpass and the corresponding satellite image as an indication of the colocation uncertainty due to iceberg drift; Negative values indicate that the image was taken before the CryoSat overpass. m~~a~~) mean difference of each new overpass along time. CryoSat-2 tracks that have been ~~geolocated~~ colocated are marked with a diamond, but all available CryoSat-2 overpasses have been used to calculate a moving mean and fit a polynomial; The shading shows the standard deviations. ~~b m) freeboard difference in each grid cell sampled by geolocated CryoSat-2 overpasses; the Δt values give the time difference between the CryoSat-2 overpass and the corresponding satellite image as an indication of the geolocation uncertainty due to iceberg drift;~~ n) scatter plot of freeboard change from ~~geolocated~~ colocated CryoSat-2 tracks versus the same tracks used without ~~geolocation~~ colocation

3.3 Iceberg t~~T~~hickness c~~C~~hange

We compute the iceberg thickness from our measurements of its freeboard (using the moving mean, red line in Fig. 7m) and by assuming that it is floating in hydrostatic equilibrium within the surrounding ocean with a surface snow layer. Accounting for the snow layer is important because it affects the ice freeboard and the iceberg buoyancy, and we take both effects into consideration. Based on hourly snowfall, evaporation and snowmelt derived from ERA5 reanalyses (Copernicus Climate Change Service, 2018), we estimate that the iceberg accumulates 4.6 m of snow water equivalent during the 6.5 year survey period (Fig. 8). The rate of accumulation is quite linear. The iceberg thickness also depends on densities of the snow layer, the iceberg, and the sea-water and we allow the snow layer and iceberg densities to evolve over time due to the changing environmental conditions it experiences during its long lifecycle. The mean iceberg density reduces from an initial estimate of 864 kg m^{-3} to a final value of 835 kg m^{-3} as a consequence of basal ice melting (Fig. 8a). The mean firn densification in West Antarctica has been estimated to be 2.78 cm per year on floating ice (Zwally et al., 2005); ~~applying~~ upscaling this rate gives a total of 18 cm after 6.5 years, which is significantly smaller than the observed freeboard loss of 9.2 m, so we don't apply it. The snow layer compacts over time due to its accumulation and warming, and we estimate that its average density rises from 252 to 616 kg m^{-3} which yields a 7.2 m thick layer after 6.5 years (Fig. 8b). We also investigate the impact of surface thawing; although the iceberg surface does experience temperatures above freezing every summer and for a total of 218 degree hours (number of hours above zero degrees Celsius times the temperature above zero degrees Celsius) since calving (Fig. 8c), in situ observations (Scambos et al., 2008) suggest that this translates into only 8 to 16 cm of snow melting and this has negligible impact on the iceberg freeboard, so we discard this effect.

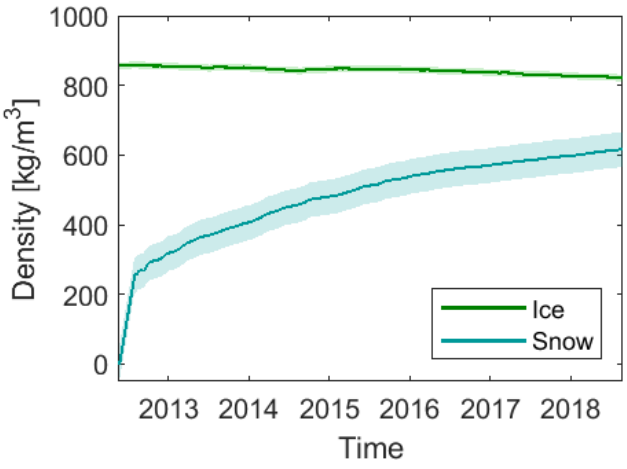
Density [kg/m^3]
1000
800
600
400
200
0
2013 2014 2015 2016 2017 2018
Time
Ice
Snow

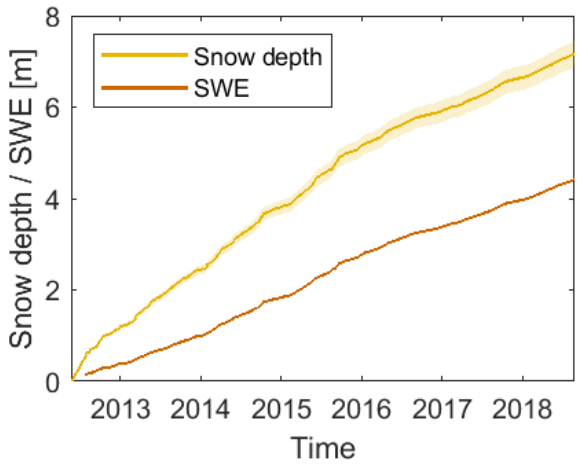
Snow depth / SWE [m]
8
6
4
2
0
2013 2014 2015 2016 2017 2018
Time
Snow depth
SWE

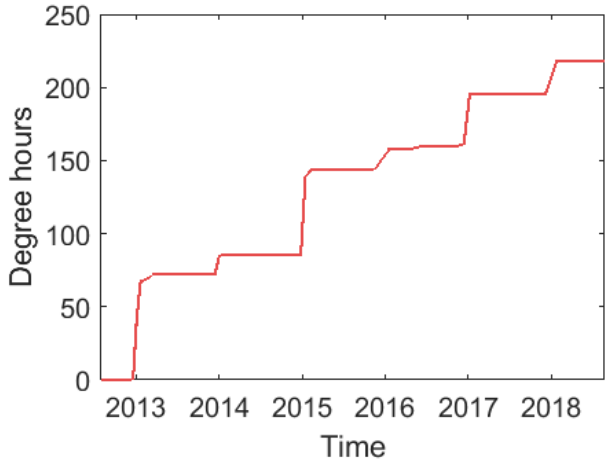
Degree hours
250
200
150
100
50
0
2013 2014 2015 2016 2017 2018
Time

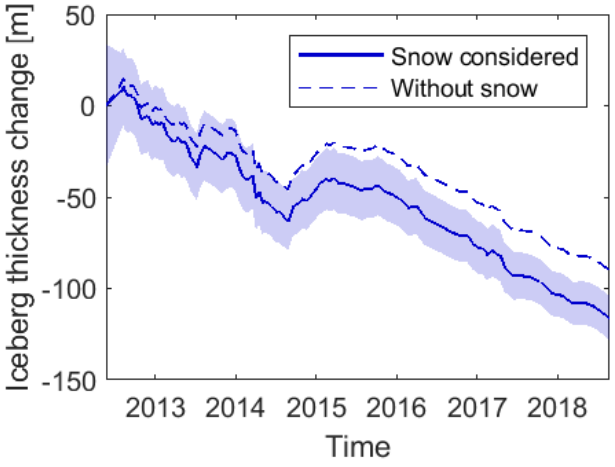
Iceberg thickness change [m]
50
0
-50
-100
-150
2013 2014 2015 2016 2017 2018
Time
Snow considered
Without snow

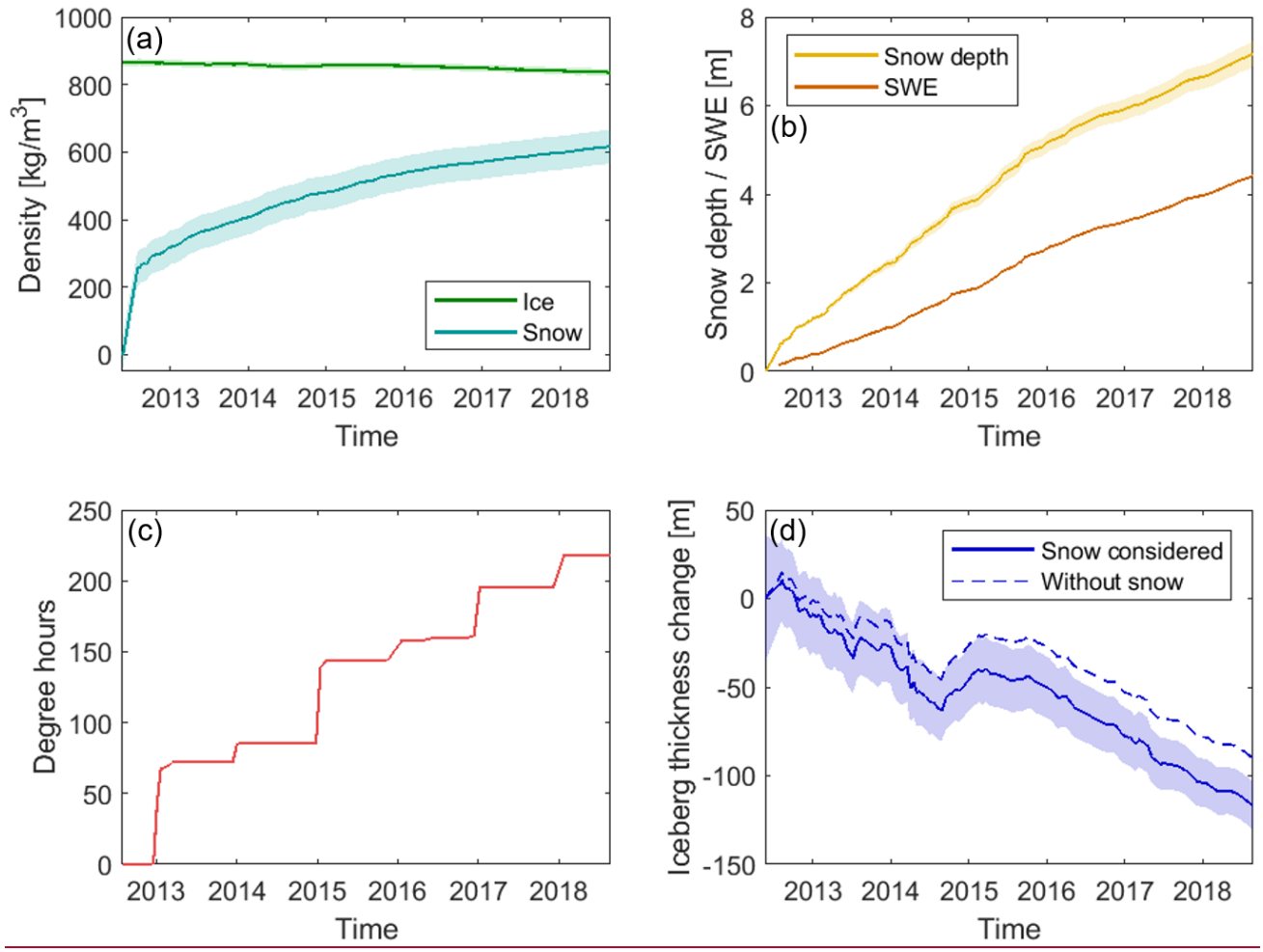

Figure 8: Evolution of the B30 iceberg properties: a) Ice density and snow density, b) Snow water equivalent (SWE) and snow depth accumulation on the B30 iceberg, c) Degree hours that the B30 iceberg experienced and d) Thickness change of the B30 iceberg with snow accumulation taken into consideration or without. Uncertainties are plotted as shaded areas.

We estimate the initial iceberg thickness to be 315 ± 36 m, on average, reducing to 198 ± 14 m after 6.5 years ~~(Fig. 8d)~~. This amounts to 117 ± 38 m of thinning (Fig. 8d) at an average rate of 17.3 ± 1.8 m per year. Previous studies have recorded iceberg thinning rates of up to 10 m per year when drifting within the sea ice extent close to the coast (Han et al., 2019; Jansen et al., 2007; Li et al., 2018; Scambos et al., 2008) and much higher rates in excess of 20 m per year when in warmer open water (Hamley and Budd, 1986; Jansen et al., 2007; Li et al., 2018; Scambos et al., 2008; Tournadre et al., 2015). The B30 iceberg has spent most of its lifetime close to the coast (Fig. 1), and so our estimated average thinning rate is in line with the results from other studies. To assess the impact of including a snow layer in the thickness calculation, we also

compute thickness change assuming no snow has accumulated since calving (Fig. 8d); this scenario leads to an estimated 90 ± 39 m reduction in iceberg thickness, 23 % lower than the rate determined when the snow layer is included, which illustrates its importance. Based on the mostly linear snow accumulation, we expect the importance of including a snow layer to be highest in phases where the iceberg is melting slowly, as snow accumulation can disguise the thickness change in this instance. It will also be more important the longer the iceberg survives, as more snow accumulates. Apart from the snow layer, the iceberg density is also a significant factor in our thickness change calculation, and while we have attempted to model the evolutions of ice density, snow density, snow accumulation and surface thawing, their uncertainties are difficult to quantify.

Besides the observed thinning, the iceberg also seems to slightly thicken between mid-2014 and early 2015. During this time B30 was very close to the coast (Fig. 3b-d). Therefore, a range of processes – both physical processes that impact the actual thickness of the iceberg and processes that impact the freeboard measurement – could have caused this gain in thickness: First of all, iceberg thickness can increase through marine ice formation, when the iceberg is surrounded by very cold water. It can also grow through snow accumulation on the surface, which we account for, but only based on reanalysis data and there might be additional local snowfall or snow accumulation through strong katabatic winds from the near-by continent. Furthermore, external forcing from fast ice and/or collisions with the adjacent ice-shelf might have led to a deformation and hence a compression in some parts. All of these processes can cause a physical increase in iceberg thickness. Apart from that, a short (partial) grounding could lead to higher measured iceberg freeboards. Also surface melting could shift the scattering horizon of CryoSat-2 and therefore appear like a freeboard increase. Indeed we observe a steep increase in degree hours around the turn of the year 2015. What caused the signal in this instance is hard to disentangle. Most probably, it was a combination of several of the mentioned effects.

3.4 Iceberg v~~V~~olume and m~~M~~ass c~~C~~hange

Having calculated changes in the B30 iceberg thickness associated with snowfall and basal melting and changes in area due to fragmentation, we combine both to determine the overall change in volume (Fig. 9). To do this, we multiply each thickness estimate ~~(Fig. 8d)~~ with the imagery-based area estimates ~~(Fig. 6)~~ interpolated to the times of the CryoSat-2 overpasses. The proportion of the total volume changes associated with melting and fragmentation are calculated by keeping area and thickness constant (and equal to their average), respectively. To compute changes in mass, we multiply the volume change due to fragmentation by the column-average iceberg density at each point in time, because this ice is lost at the sides. In contrast, we multiply the volume change due to basal melting by the density of pure ice (915 kg m^{-3}), since this ice is lost at the bottom where ice density is highest. The total mass change is the sum of both components. Uncertainties are calculated by propagating the uncertainties of thickness change, area change and ice density.

The initial volume of B30 at the time of its calving was 472 ± 57 km^3 and after 6.5 years it has lost 378 ± 57 km^3 of ice, corresponding to a 80 ± 16 % reduction. Fragmentation accounts for two thirds (69 ± 14 %) of the total volume loss and basal melting is responsible for the remainder (31 ± 11 %). However, volume changes due to fragmentation become the dominant source of ice loss towards the end of our survey, consistent with previous findings (Bouhier et al., 2018). This is because the main drivers of fragmentation are surface melting, which can lead to a rapid disintegration (Scambos et al., 2008) and wave erosion or wave stress (Wagner et al., 2014) which increase the further North (i.e. surrounded by open ocean and warmer air temperatures) the iceberg gets. The two icebergs studied by Bouhier et al., (2018) also show similar fractions of ice loss due to fragmentation (60% for the B17a iceberg and 75% for the C19a iceberg). In terms of mass, the iceberg has lost 325 ± 44 Gt of ice in total at an average rate of 46 ± 4 Gt per year. The loss due to basal melting (106 ± 35 Gt) can be used as a lower estimate of the freshwater flux from B30. Some of the mass lost due to changes in area - in particular melting at the sides and smaller edge wastings - will probably melt locally and add to the freshwater flux, but bigger calving events create smaller icebergs which can survive and travel on their own (England et al., 2020; Martin and Adcroft, 2010). To calculate the total freshwater flux, the melting of all fragments has to be considered.

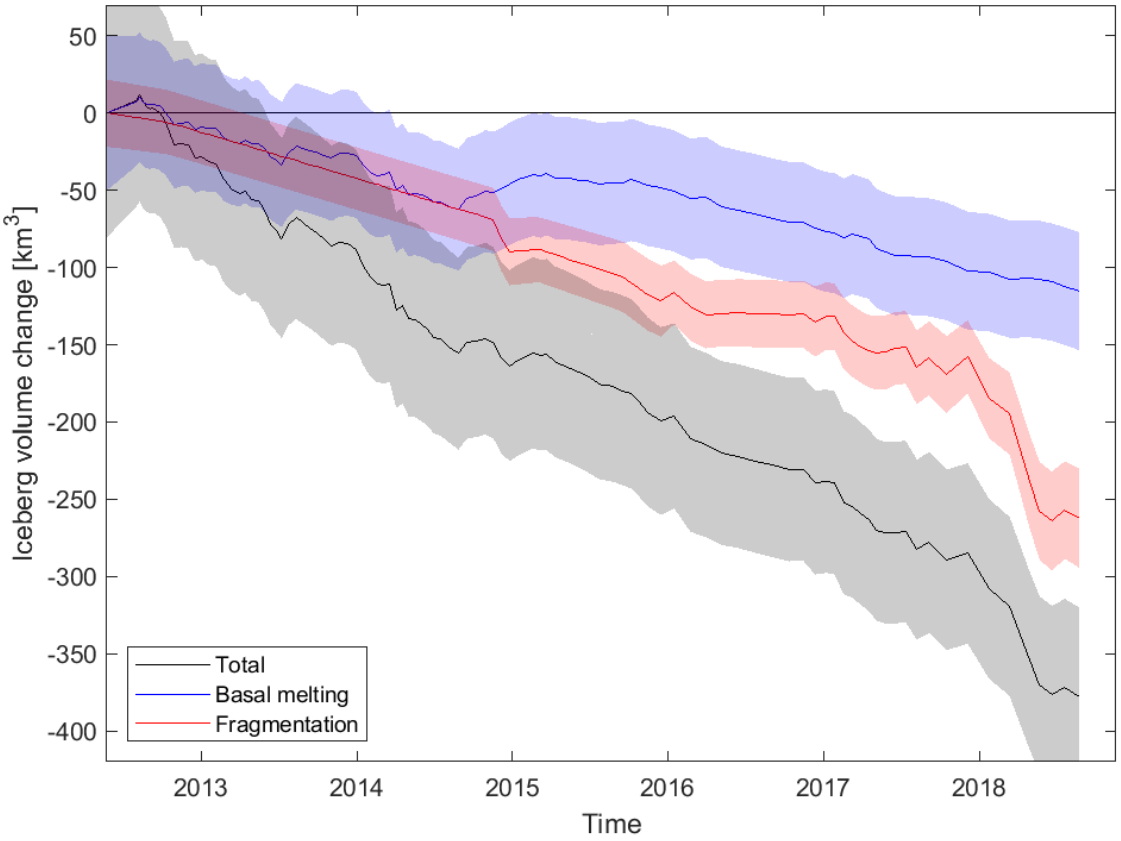

Figure 9: Volume change of the B30 iceberg divided into loss due to basal melting (thickness change, blue) and due to fragmentation (area change, red), as well as total volume loss (black).

4 Conclusions

In this study we have derived changes in the area, freeboard, thickness, and volume of the B30 iceberg using a combination of satellite altimetry and satellite imagery. During the 6.5 years after the iceberg calved in May 2012, its area reduced from 1500 ± 60 km^2 to 426 ± 27 km^2 at an average rate of 149 ± 5 km^2 per year. The iceberg freeboard lowered by 9.2 ± 2.2 m over the same period. Using estimates of the snow accumulation and changes in snow and ice density, we estimate that the iceberg thinned by 117 ± 38 m at a mean rate of 17.3 ± 1.8 m per year. Altogether, the iceberg lost 378 ± 57 km^3 of ice, and this equates to an estimated 325 ± 44 Gt reduction in mass.

We investigated the capability of automated approaches to approximate iceberg area and area change by comparing them to manually-derived estimates. Although the most reliable method of charting iceberg area change is through manual delineation in satellite imagery, we show that less time-consuming estimates derived from measurements of the iceberg's orthogonal axes or arc-lengths are also able to capture the area and area change over time, albeit with poorer certainty. Orthogonal axes lead to estimates of area and area trends that are 14 % and 16 % higher, respectively, and arc-lengths lead to estimates of area and area trends that are 45% and 48% lower, due to the necessary approximate of the iceberg shape.

We also presented a new thorough methodology to investigate iceberg freeboard and thickness change, using a densely sampled time series of consistently processed Level 1 CryoSat data and assessed the importance of ~~geolocation~~colocation. Using a subset of 12 instances with ~~geolocation~~colocation, we find that omitting this step leads to a small deterioration in the certainty of detected freeboard change for the B30 iceberg, but the densely sampled time series is in good agreement with the ~~geolocated~~ colocated tracks. We expect this finding also holds for other large tabular Antarctic icebergs with uniform topography, when the observed freeboard change exceeds the topography and when enough tracks are averaged. In this case, it suggests that the procedure for tracking changes in iceberg thickness could be automated, given reliable estimates of their position (Budge and Long, 2018).

Finally, we developed a methodology to account for snowfall and variations in snow and ice density due to changing environmental conditions that large icebergs experience during their multi-annual drift. We found that the impact of snowfall on the retrieval of iceberg thickness increases over time, and after 6.5 years we estimate that 7.2 metres of snow have accumulated which leads to a 27 m adjustment to the iceberg thickness change. Iceberg thickness change is also strongly dependent on the density profile which we derive from the depths of critical density levels (Ligtenberg et al., 2011), and so in situ observations would help to assess the reliability of this relationship. Likewise, direct measurements of the near-surface firn will help to assess the reliability of our reanalyses-based estimate of snow loading.

More icebergs - including the fragments lost from B30 - need to be studied to generalise the results we have and to constrain both the fresh water flux, which influences water circulation (Grosfeld et al., 2001; Jenkins, 1999) and promotes sea ice formation (Bintanja et al., 2015; Merino et al., 2016), and input of terrigenous nutrients such as glacial iron into the Southern Ocean, which fosters primary production (Biddle et al., 2015; Duprat et al., 2016; Helly et al., 2011). Finally, studying icebergs as they drift through warmer water may give unique insights into the response of glacial ice to environmental conditions which may become commonplace at the ice shelf front in the future (Scambos et al., 2008; Shepherd et al., 2019).

Code availability

The code (mostly written in matlab) is available from the authors upon reasonable request.

Data availability

All data used in this study is freely available: The iceberg trajectory data is available from https://www.scp.byu.edu/data/iceberg/, CryoSat-2 data is available from https://science-pds.cryosat.esa.int/, Sentinel-1 data from https://scihub.copernicus.eu/dhus/, MODIS data from https://ladsweb.modaps.eosdis.nasa.gov/search/order/1/MOD02HKM--61 and the ERA-5 reanalysis data from https://cds.climate.copernicus.eu/cdsapp#!/dataset/reanalysis-era5-single-levels.

Author contributions

ABF and AS designed the study, AR processed the CryoSat elevations, ABF computed freeboard, area and volume change and prepared the figures, AS supervised the work. All authors contributed to the writing.

Competing interests

The authors declare that they have no conflict of interest.

Acknowledgements

This work was supported by Barry Slavin and the Centre for Polar Observation and Modelling. The Antarctic Mapping Toolbox (Greene et al., 2017) was used to convert geographic coordinates to polar stereographic and vice versa and to calculate distances. We thank the anonymous reviewer and Jessica Scheick for their detailed reviews and Xuying Liu for a short comment, which all helped to improve the manuscript.

References

Arrigo, K. R., Van Dijken, G. L., Ainley, D. G., Fahnestock, M. A. and Markus, T.: Ecological impact of a large Antarctic iceberg, Geophys. Res. Lett., 29(7), 8-1-8–4, https://doi.org/10.1029/2001GL014160, 2002.

Barnes, D. K. A.: Iceberg killing fields limit huge potential for benthic blue carbon in Antarctic shallows, Glob. Chang.

Biol., 23(7), 2649–2659, https://doi.org/10.1111/gcb.13523, 2017.

Biddle, L. C., Kaiser, J., Heywood, K. J., Thompson, A. F. and Jenkins, A.: Ocean glider observations of iceberg-enhanced biological production in the northwestern Weddell Sea, Geophys. Res. Lett., 42(2), 459–465, https://doi.org/10.1002/2014GL062850, 2015.

Bigg, G. R., Cropper, T. E., O'Neill, C. K., Arnold, A. K., Fleming, A. H., Marsh, R., Ivchenko, V., Fournier, N., Osborne, M. and Stephens, R.: A model for assessing iceberg hazard, Nat. Hazards, 92(2), 1113–1136, https://doi.org/10.1007/s11069-018-3243-x, 2018.

Bintanja, R., Van Oldenborgh, G. J. and Katsman, C. A.: The effect of increased fresh water from Antarctic ice shelves on future trends in Antarctic sea ice, Ann. Glaciol., 56(69), 120–126, https://doi.org/10.3189/2015AoG69A001, 2015.

Bouhier, N., Tournadre, J., Rémy, F. and Gourves-Cousin, R.: Melting and fragmentation laws from the evolution of two large Southern Ocean icebergs estimated from satellite data, Cryosphere, 12(7), 2267–2285, https://doi.org/10.5194/tc-12-2267-2018, 2018.

Budge, J. S. and Long, D. G.: A Comprehensive Database for Antarctic Iceberg Tracking Using Scatterometer Data, IEEE J. Sel. Top. Appl. Earth Obs. Remote Sens., 11(2), 434–442, https://doi.org/10.1109/JSTARS.2017.2784186, 2018.

Copernicus Climate Change Service, C.: ERA5 hourly data on single levels from 1979 to present, , https://doi.org/10.24381/cds.adbb2d47, 2018.

Dammann, D. O., Eriksson, L. E. B., Nghiem, S. V., Pettit, E. C., Kurtz, N. T., Sonntag, J. G., Busche, T. E., Meyer, F. J. and Mahoney, A. R.: Iceberg topography and volume classification using TanDEM-X interferometry, Cryosphere, 13(7), 1861–1875, https://doi.org/10.5194/tc-13-1861-2019, 2019.

Depoorter, M. A., Bamber, J. L., Griggs, J. A., Lenaerts, J. T. M., Ligtenberg, S. R. M., Van Den Broeke, M. R. and Moholdt, G.: Calving fluxes and basal melt rates of Antarctic ice shelves, Nature, 502(7469), 89–92, https://doi.org/10.1038/nature12567, 2013.

Duprat, L. P. A. M., Bigg, G. R. and Wilton, D. J.: Enhanced Southern Ocean marine productivity due to fertilization by giant icebergs, Nat. Geosci., 9(3), 219–221, https://doi.org/10.1038/ngeo2633, 2016.

Eik, K. and Gudmestad, O. T.: Iceberg management and impact on design of offshore structures, Cold Reg. Sci. Technol., 63(1–2), 15–28, https://doi.org/10.1016/j.coldregions.2010.04.008, 2010.

Enderlin, E. M. and Hamilton, G. S.: Estimates of iceberg submarine melting from high-resolution digital elevation models: Application to Sermilik Fjord, East Greenland, J. Glaciol., 60(224), 1111–1116, https://doi.org/10.3189/2014JoG14J085, 2014.

England, M. R., Wagner, T. J. W. and Eisenman, I.: Modeling the breakup of tabular icebergs, Sci. Adv., 6(51), 1–9, https://doi.org/10.1126/sciadv.abd1273, 2020.

Fichefet, T. and Morales Maqueda, M. A.: Modelling the influence of snow accumulation and snow-ice formation on the seasonal cycle of the Antarctic sea-ice cover, Clim. Dyn., 15(4), 251–268, https://doi.org/10.1007/s003820050280, 1999.

Gladstone, R. M., Bigg, G. R. and Nicholls, K. W.: Iceberg trajectory modeling and meltwater injection in the Southern Ocean, J. Geophys. Res. Ocean., 106(C9), 19903–19915, https://doi.org/10.1029/2000jc000347, 2001.

Greene, C. A., Gwyther, D. E. and Blankenship, D. D.: Antarctic Mapping Tools for MATLAB, Comput. Geosci., 104, 151–157, https://doi.org/10.1016/j.cageo.2016.08.003, 2017.

Grosfeld, K., Schröder, M., Fahrbach, E., Gerdes, R. and Mackensen, A.: How iceberg calving and grounding change the circulation and hydrography in the Filchner Ice Shelf–Ocean System, J. Geophys. Res., 106(2000), 9039–9055, 2001.

Gutt, J.: On the direct impact of ice on marine benthic communities, a review, Polar Biol., 24(8), 553–564, https://doi.org/10.1007/s003000100262, 2001.

Hamley, T. C. and Budd, W. F.: Antarctic Iceberg Distribution and Dissolution, J. Glaciol., 32(111), 242–251, https://doi.org/10.1017/s0022143000015574, 1986.

Han, H., Lee, S., Kim, J. I., Kim, S. H. and Kim, H. C.: Changes in a giant iceberg created from the collapse of the Larsen C Ice Shelf, Antarctic Peninsula, derived from Sentinel-1 and CryoSat-2 data, Remote Sens., 11(4), 1–14, https://doi.org/10.3390/rs11040404, 2019.

Helly, J. J., Kaufmann, R. S., Stephenson, G. R. and Vernet, M.: Cooling, dilution and mixing of ocean water by free-drifting icebergs in the Weddell Sea, Deep. Res. Part II Top. Stud. Oceanogr., 58(11–12), 1346–1363, https://doi.org/10.1016/j.dsr2.2010.11.010, 2011.

Huppert, H. E. and Josberger, E. G.: The Melting of Ice in Cold Stratified water, J. Phys. Oceanogr., 1980.

International Organization for Standardization, I.: ISO 4355 Bases for design on structures – Determination of snow loads on roofs., 1998.

Jansen, D., Schodlok, M. and Rack, W.: Basal melting of A-38B: A physical model constrained by satellite observations, Remote Sens. Environ., 111(2), 195–203, https://doi.org/10.1016/j.rse.2007.03.022, 2007.

Jenkins, A.: The impact of melting ice on ocean waters, J. Phys. Oceanogr., 29(9), 2370–2381, https://doi.org/10.1175/1520-0485(1999)029<2370:TIOMIO>2.0.CO;2, 1999.

Joiris, C. R.: Seabird hotspots on icebergs in the Amundsen Sea, Antarctica, Polar Biol., 41(1), 111–114, https://doi.org/10.1007/s00300-017-2174-4, 2018.

Jongma, J. I., Driesschaert, E., Fichefet, T., Goosse, H. and Renssen, H.: The effect of dynamic-thermodynamic icebergs on the Southern Ocean climate in a three-dimensional model, Ocean Model., 26(1–2), 104–113, https://doi.org/10.1016/j.ocemod.2008.09.007, 2009.

Kooyman, G. L., Ainley, D. G., Ballard, G. and Ponganis, P. J.: Effects of giant icebergs on two emperor penguin colonies

in the Ross Sea, Antarctica, Antarct. Sci., 19(1), 31–38, https://doi.org/10.1017/S0954102007000065, 2007.

Kurtz, N. T. and Markus, T.: Satellite observations of Antarctic sea ice thickness and volume, J. Geophys. Res. Ocean., 117(8), 1–9, https://doi.org/10.1029/2012JC008141, 2012.

Laufkötter, C., Stern, A. A., John, J. G., Stock, C. A. and Dunne, J. P.: Glacial Iron Sources Stimulate the Southern Ocean Carbon Cycle, Geophys. Res. Lett., 45(24), 13,377-13,385, https://doi.org/10.1029/2018GL079797, 2018.

Li, T., Shokr, M., Liu, Y., Cheng, X., Li, T., Wang, F. and Hui, F.: Monitoring the tabular icebergs C28A and C28B calved from the Mertz Ice Tongue using radar remote sensing data, Remote Sens. Environ., 216(July 2017), 615–625, https://doi.org/10.1016/j.rse.2018.07.028, 2018.

Ligtenberg, S. R. M., Helsen, M. M. and Van Den Broeke, M. R.: An improved semi-empirical model for the densification of Antarctic firn, Cryosphere, 5(4), 809–819, https://doi.org/10.5194/tc-5-809-2011, 2011.

Martin, T. and Adcroft, A.: Parameterizing the fresh-water flux from land ice to ocean with interactive icebergs in a coupled climate model, Ocean Model., 34(3–4), 111–124, https://doi.org/10.1016/j.ocemod.2010.05.001, 2010.

Mazur, A. K., Wåhlin, A. K. and Kalén, O.: The life cycle of small-to medium-sized icebergs in the Amundsen sea embayment, Polar Res., 38, 1–17, https://doi.org/10.33265/polar.v38.3313, 2019.

McIntyre, N. F. and Cudlip, W.: Observation of a giant antarctic tabular iceberg by satellite radar altimetry, Polar Rec. (Gr. Brit)., 23(145), 458–462, https://doi.org/10.1017/S0032247400007610, 1987.

Merino, N., Le Sommer, J., Durand, G., Jourdain, N. C., Madec, G., Mathiot, P. and Tournadre, J.: Antarctic icebergs melt over the Southern Ocean : Climatology and impact on sea ice, Ocean Model., 104, 99–110, https://doi.org/10.1016/j.ocemod.2016.05.001, 2016.

Moon, T., Sutherland, D. A., Carroll, D., Felikson, D., Kehrl, L. and Straneo, F.: Subsurface iceberg melt key to Greenland fjord freshwater budget, Nat. Geosci., 11(1), 49–54, https://doi.org/10.1038/s41561-017-0018-z, 2018.

Mouginot, J., Rignot, E. and Scheuchl, B.: Continent-Wide, Interferometric SAR Phase, Mapping of Antarctic Ice Velocity, Geophys. Res. Lett., 46(16), 9710–9718, https://doi.org/10.1029/2019GL083826, 2019.

Neshyba, S. and Josberger, E. G.: On the estimation of Antarctic iceberg melt rate, J. Phys. Oceanogr., 1980.

Nøst, O. A. and Østerhus, S.: Impact of Grounded Icebergs on the Hydrographic Conditions Near the Filchner Ice Shelf, , 75, 267–284, https://doi.org/10.1029/ar075p0267, 2013.

Rackow, T., Wesche, C., Timmermann, R., Hellmer, H. H., Juricke, S. and Jung, T.: A simulation of small to giant Antarctic iceberg evolution: Differential impact on climatology estimates, J. Geophys. Res. Ocean., 3170–3190, https://doi.org/10.1002/2016JC012513.Received, 2013.

Raiswell, R., Hawkings, J. R., Benning, L. G., Baker, A. R., Death, R., Albani, S., Mahowald, N., Krom, M. D., Poulton, S. W., Wadham, J. and Tranter, M.: Potentially bioavailable iron delivery by iceberg-hosted sediments and atmospheric

dust to the polar oceans, Biogeosciences, 13(13), 3887–3900, https://doi.org/10.5194/bg-13-3887-2016, 2016.

Remy, J. P., Becquevort, S., Haskell, T. G. and Tison, J. L.: Impact of the B-15 iceberg "stranding event" on the physical and biological properties of sea ice in McMurdo Sound, Ross Sea, Antarctica, Antarct. Sci., 20(6), 593–604, https://doi.org/10.1017/S0954102008001284, 2008.

Rignot, E., Jacobs, S., Mouginot, J. and Scheuchl, B.: Ice-shelf melting around antarctica, Science (80-.)., 341(6143), 266–270, https://doi.org/10.1126/science.1235798, 2013.

Robinson, N. J. and Williams, M. J. M.: Iceberg-induced changes to polynya operation and regional oceanography in the southern Ross Sea, Antarctica, from in situ observations, Antarct. Sci., 24(5), 514–526, https://doi.org/10.1017/S0954102012000296, 2012.

Russell-Head, D. S.: The Melting of Free-Drifting Icebergs, Ann. Glaciol., 1, 119–122, https://doi.org/10.3189/s0260305500017092, 1980.

Scambos, T., Ross, R., Bauer, R., Yermolin, Y., Skvarca, P., Long, D., Bohlander, J. and Haran, T.: Calving and ice-shelf break-up processes investigated by proxy: Antarctic tabular iceberg evolution during northward drift, J. Glaciol., 54(187), 579–591, https://doi.org/10.3189/002214308786570836, 2008.

Schloesser, F., Friedrich, T., Timmermann, A., DeConto, R. M. and Pollard, D.: Antarctic iceberg impacts on future Southern Hemisphere climate, Nat. Clim. Chang., 9(9), 672–677, https://doi.org/10.1038/s41558-019-0546-1, 2019.

Shepherd, A., Gilbert, L., Muir, A. S., Konrad, H., McMillan, M., Slater, T., Briggs, K. H., Sundal, A. V., Hogg, A. E. and Engdahl, M. E.: Trends in Antarctic Ice Sheet Elevation and Mass, Geophys. Res. Lett., 46(14), 8174–8183, https://doi.org/10.1029/2019GL082182, 2019.

Silva, T. A. M., Bigg, G. R. and Nicholls, K. W.: Contribution of giant icebergs to the Southern Ocean freshwater flux, , 111(July 2005), 1–8, https://doi.org/10.1029/2004JC002843, 2006.

Smith, K. L., Robison, B. H., Helly, J. J., Kaufmann, R. S., Ruhl, H. A., Shaw, T. J., Twining, B. S. and Vernet, M.: Free-drifting icebergs: Hot spots of chemical and biological enrichment in the Weddell Sea, Science (80-.)., 317(5837), 478–482, https://doi.org/10.1126/science.1142834, 2007.

Sulak, D. J., Sutherland, D. A., Enderlin, E. M., Stearns, L. A. and Hamilton, G. S.: Iceberg properties and distributions in three Greenlandic fjords using satellite imagery, Ann. Glaciol., 58(74), 92–106, https://doi.org/10.1017/aog.2017.5, 2017.

Tilling, R. L., Ridout, A. and Shepherd, A.: Estimating Arctic sea ice thickness and volume using CryoSat-2 radar altimeter data, Adv. Sp. Res., 62(6), 1203–1225, https://doi.org/10.1016/j.asr.2017.10.051, 2018.

Tournadre, J., Bouhier, N., Girard-Ardhuin, F. and Remy, F.: Large icebergs characteristics from altimeter waveforms analysis, J. Geophys. Res. Ocean., (Mcl), 2121–2128, https://doi.org/10.1002/jgrc.20224, 2015.

Wagner, T. J. W., Wadhams, P., Bates, R., Elosegui, P., Stern, A., Vella, D., Abrahamsen, E. P., Crawford, A. and Nicholls,

650 K. W.: The “footloose” mechanism: Iceberg decay from hydrostatic stresses, Geophys. Res. Lett., 41(15), 5522–5529, https://doi.org/10.1002/2014GL060832, 2014.

Wise, M. G., Dowdeswell, J. A., Jakobsson, M. and Larter, R. D.: Evidence of marine ice-cliff instability in Pine Island Bay from iceberg-keel plough marks, Nature, 550(7677), 506–510, https://doi.org/10.1038/nature24458, 2017.

Wu, S. Y. and Hou, S.: Impact of icebergs on net primary productivity in the Southern Ocean, Cryosphere, 11(2), 707–
655 722, https://doi.org/10.5194/tc-11-707-2017, 2017.

Zwally, H. J., Giovinetto, M. B., Li, J., Cornejo, H. G., Beckley, M. A., Brenner, A. C., Saba, J. L. and Yi, D.: Mass changes of the Greenland and Antarctic ice sheets and shelves and contributions to sea-level rise: 1992-2002, J. Glaciol., 51(175), 509–527, https://doi.org/10.3189/172756505781829007, 2005.